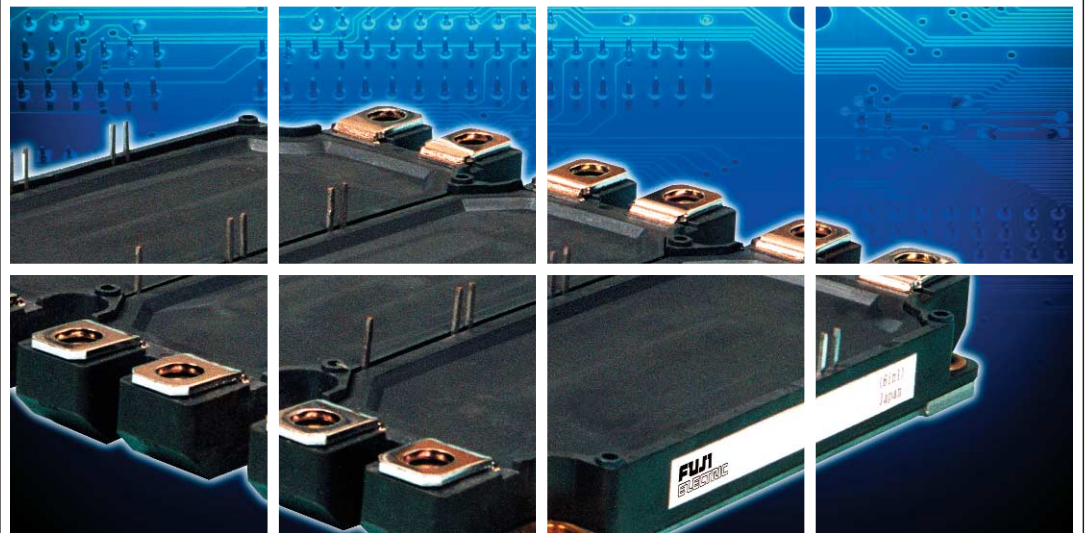
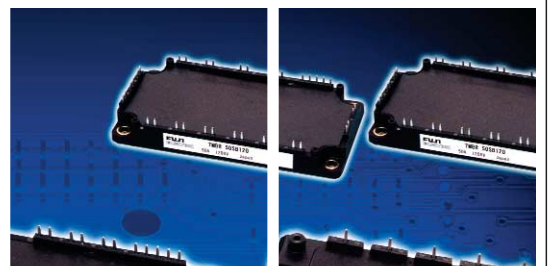


FUJI ELECTRIC REVIEW



2002 VOL.48

Power Semiconductors



A slimmer package enables thinner and smaller servo amps



■ Features of the 600V Econo IPM for servo amp applications

- Use of 600V NPT-IGBT allows switching loss to be decreased
- Use of new diode allows FWD recovery dv/dt to be decreased
- Small, thin package
 - Slimmer IPM package [width reduced to 55mm from 88mm (prior)]
 - Reduced height of printed circuit board [height reduced to 17mm from 22mm (prior)]
 - Same package as converter module (Product lineup also includes Econo Diode Module)
- Secure and safe operation
 - Upper arm alarm output pin has been added
 - Overvoltage protection provided by current sensing function (same as R-IPM)
 - Overheating protection provided by on-chip temperature sensor (same as R-IPM)
- High reliability
 - Improved power cycle performance

Econo IPM Series Dimensions: 122 (L) × 55 (W) × 17 (H) mm

No. of devices	Model	V_{CES} (V)	Inverter unit		
			I_C (A)	$V_{CE(sat)}$ typ. (V)	V_F typ. (V)
6in1	6MBP 50TEA060	600	50	2.1	1.7
	6MBP 75TEA060	600	75	2.1	1.7
	6MBP100TEA060	600	100	2.0	1.7
	6MBP150TEA060	600	150	2.0	1.7
7in1	7MBP 50TEA060	600	50	2.1	1.7
	7MBP 75TEA060	600	75	2.1	1.7
	7MBP100TEA060	600	100	2.0	1.7
	7MBP150TEA060	600	150	2.0	1.7

Built-in protection functions:
 Overcurrent protection, Short circuit protection, IGBT chip overheat protection,
 Control power supply brownout protection, Upper and lower arm alarm outputs

Quality is our message

Fuji Intelligent Power Module Econo IPM Series

FUJI ELECTRIC REVIEW

Power Semiconductors

4

2002 VOL.48

CONTENTS

Present Status and Trends of Power Semiconductor Devices	102
Technological Innovation for Super-low-loss U-series IGBT Modules	106
T-series and U-series IGBT Modules (600 V)	110
U-series IGBT Modules (1,200 V)	115
U-series IGBT Modules (1,700 V)	120
R-IPM3 and Econo IPM Series of Intelligent Power Modules	125
SuperFAP-G Series of Power MOSFETs	131

Cover photo:

Power semiconductor modules, a core element of power electronics technology, are being used by new electric power control techniques in a wide range of devices having diverse capacities, and in this manner, are making a beneficial contribution to society.

Fuji Electric, leveraging its leading-edge semiconductor technology, has always been a leader in this industry and has a history of supplying highly reliable power semiconductor modules to the market. In response to customer needs, Fuji Electric has recently commercialized a diversified product series of 5th generation IGBT modules. The superior characteristics of these modules are receiving widespread attention in the marketplace.

The cover photograph shows 5th generation IGBT modules, which range from small capacity to large capacity modules, and our corporate logo, "*Quality is our message*," expressing our commitment to consistently high quality.

Present Status and Trends of Power Semiconductor Devices

Hisao Shigekane
Yasukazu Seki
Tatsuhiko Fujihira

1. Introduction

In the midst of prolonged economic stagnation and sluggish economic conditions, demand for technological development is still strong, and it is our belief that technological development will steadily advance in the future. With a concerted drive toward technological development, we have been building up the infrastructure of our society in order to realize a better future.

At present, one of the major technologies supporting such technological development is power electronics, which is widely used in almost every field of our daily life. Fuji Electric has vigorously been developing power devices, the basis of power electronics technology. With the advances in power electronics technology, higher reliability as well as enhanced functionality and higher performance has come to be required of power devices.

To meet these demands, Fuji Electric is leveraging its sophisticated technological development expertise to provide highly reliable, leading-edge power devices.

2. Recent Trends of Power Device Development

The latest trends of power devices can be found in the trends of the ISPSD (International Symposium on Power Semiconductor Devices & ICs), the leading authoritative international academic society for power devices. The ISPSD was established in Japan in 1988 under the sponsorship of the Institute of Electrical Engineers of Japan (IEE) and has been promoted by engineers concerned with power devices. The annual ISPSD conference rotates between Japan, the United States and Europe. In Japan, the conference is sponsored jointly by the IEE and IEEE, and in the U.S. and Europe it is sponsored by the IEEE. ISPSD'01 was held in Osaka, Japan in 2001. In the banquet keynote address, Mr. Kunihiko Sawa, president of Fuji Electric Co., Ltd., delivered a lecture titled "My Experiences in Developments of Power Electronics — What I expect to young researchers and engineers —," based on his experiences in the development of power electronics.⁽¹⁾ The lecture made a great impression on many participants, researchers and engineers, and is

still fresh in our collective memories.

ISPSD'02 was held in Santa Fe, New Mexico in early June 2002. There were 40 oral and 31 poster presentations. Fuji Electric made three oral presentations.⁽²⁾⁻⁽⁴⁾

Table 1 shows the number of research papers presented per presentation field. From the table, it can be seen that papers on MOS-gated devices, which include IGBTs (insulated gate bipolar transistors) and MOSFETs (metal-oxide-semiconductor field effect transistors), greatly outnumber papers of other fields, and are followed by papers on Power IC/HVIC.

One reason for the keen interest in the field of power devices is the tremendous improvement in power device characteristics due to the introduction of LSI wafer process technology and because several innovative and interesting reports on power-device-specific design and process technology have been published.

In the field of recent power devices, for example, great attention is given to power-device-specific technologies such as super-junction construction with epitaxial layers of multiple thicknesses in power MOS FETs and field-stop type IGBTs with extremely thin wafers.

Another reason is the strong desire by application engineers to construct compact, highly reliable power circuit blocks that include integrated drive and protective functions in addition to the power device unit. This has resulted in the presentation of many papers related to Power IC/HVIC technology.

There is also a steady stream of presentations on SiC (silicon carbide), a new promising material. SiC is expected to be a very useful material for high-voltage power devices because SiC's maximum allowable electric field strength is approximately ten times higher than that of Si. On the other hand, there are many technical challenges to be overcome through technological innovation before SiC power devices can commercially replace Si power devices.

Table 1 Change in the number of ISPSD research papers by field during the past six years

Presentation field \ Venue	ISPSD '97 Weimar (Germany)	ISPSD '98 Kyoto (Japan)	ISPSD '99 Toronto (Canada)	ISPSD '00 Toulouse (France)	ISPSD '01 Osaka (Japan)	ISPSD '02 Santa Fe (U.S.)
Application	4	4	7	8	13	5
Simulation	6	1	1	4	1	2
Bipolar device	0	1	0	1	1	1
MOS-gated device	23	29	28	25	37	28
Power IC/HVIC	26	26	11	8	2	11
Power module	1	3	3	5	0	1
Thyristor/diode	6	12	10	8	15	4
GTO	5	6	1	0	2	0
Si device	2	3	0	0	1	0
Material/process	5	7	8	16	13	7
Packaging	2	0	1	1	6	1
SiC	8	7	6	8	11	11
Total	88	99	76	84	102	71

3. Fuji Electric's Development Policy on Power Devices

Fuji Electric is engaging in semiconductor business worldwide through marketing IGBT, power MOSFET and power diode products, concentrating on the four fields of general industry, automobile, information and consumer electronics. Fuji Electric's policy for developing new products is not to develop commodity devices for general-purpose applications but to develop products that can become the leading or the only product in limited application segments of the above four fields. Such products are referred to as killer products. Fuji Electric plans to increase its ratio of sales of killer products to total sales of semiconductors from 35 % in 2000 to 48 % in 2002.

The development of these killer products requires power device engineers to not only refine their technology but also to closely cooperate with application engineers. Fuji Electric is basically developing new products through forging strong and sustainable strategic partnerships with leading customers in various market segments. Customers do not pay money for power devices themselves, but for the results of applying such devices to electronic products. Thus, the development of new products should strive to provide device solutions that solve customers' technical problems.

Based on this viewpoint, Fuji Electric is planning to increase its sales percentage of MOS-gated devices, active devices which form the core of its device solutions, from 52 % in 2000 to 55 % in 2002, and to increase its sales percentage of smart devices and intelligent power devices, which integrate driving and protective functions into MOS-gated devices, from 28 % in 2000 to 33 % in 2002. The development of MOS-gated devices aims to combine power diodes, passive

devices, with state-of-the-art MOS-gated devices to bring about new effects in applications.

In other words, Fuji Electric's power device development policy is to develop the latest high-tech, high-performance power devices, and to provide smart and intelligent power device solutions, by combining IC technology and power devices through a concerted effort with customers.

4. Fuji Electric's IGBTs

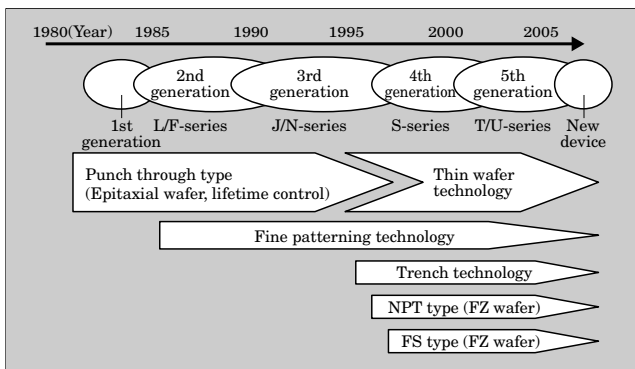
The first half of this special issue is a collection of research papers on the fifth-generation IGBT "U-series," which is subject to rapid technological innovation. These papers summarize the recently developed 600 V, 1,200 V and 1,700 V modules. For details of the U-series technological innovations, refer to the next paper, "Technological Innovation for Super-low-loss U-series IGBT modules," and for details of modules by withstand voltage, refer to the three papers thereafter.

Figure 1 shows the transition from first- to fifth-generation IGBTs and the technologies employed.

In first- to third-generation IGBTs, so-called epitaxial wafers were used to optimize lifetime control technology and to improve the IGBT performance due to micromachining technology. In fourth- and fifth-generation IGBTs, FZ (floating zone) wafers are used in place of epitaxial wafers to significantly improve performance, which resulted in drastic changes to the traditional IGBT design policy.

In designing IGBTs using epitaxial wafers, large amounts of carriers are injected at the collector side, and by means of conductivity modulation, the IGBT body is filled with carriers to achieve low on-voltage. When the current is interrupted, carriers that filled the IGBT body due to conductivity modulation are rebound together and annihilated through application of lifetime control technology. When lifetime control

Fig.1 Change in application technology for Fuji Electric's IGBTs



technology is applied, carrier transport efficiency decreases in the normal on-state due to the effect of lifetime control technology. Thus, to compensate for the reduced transport efficiency, larger amounts of carriers are injected to lower the on-voltage. The design of IGBTs using epitaxial wafers was basically involved with the principles of high carrier injection and low transport efficiency.

In designing IGBTs using FZ wafers, the basic IGBT design should be changed to suppress carrier injection at the collector side, and to increase carrier transport efficiency through reducing carrier injection efficiency. If only carrier injection efficiency is reduced, on-voltage increases. To overcome this problem, carrier transport efficiency was increased in the IGBT body. As a result, lifetime control became unnecessary. Fuji Electric started to apply this design to fourth-generation 1,200 V "S-series" IGBTs having NPT (non-punch through) structure.

The use of FZ wafers requires technology for reducing wafer thickness to achieve NPT construction, in addition to conventional semiconductor device development technology. Fuji Electric was the first to develop this technology and has actively promoted application of FZ wafers to IGBTs. Enabled by further reduction of wafer thickness, the 600 V "T-series" of IGBTs were developed.

Trench process technology at the emitter side of a chip surface is also essential for improving IGBT performance. When applying trench process technology to IGBTs, there had been a problem for some time in that on-voltage decreased but short-circuit withstand capability also decreased. Optimization of the surface design and NPT design, however, solved that problem and contributed to significant performance improvement in the 600 V fifth-generation IGBT U-series.

For further performance improvement, IGBT structure evolved from NPT to FS (field stop) structure. In FS structure, n+ buffer layers in conventional IGBTs are used as FS layers. While maintaining low carrier injection and high transport efficiency, FS layers are made thinner than those in NPT construc-

Fig.2 Change in cross-section structure of 600 V IGBT chips

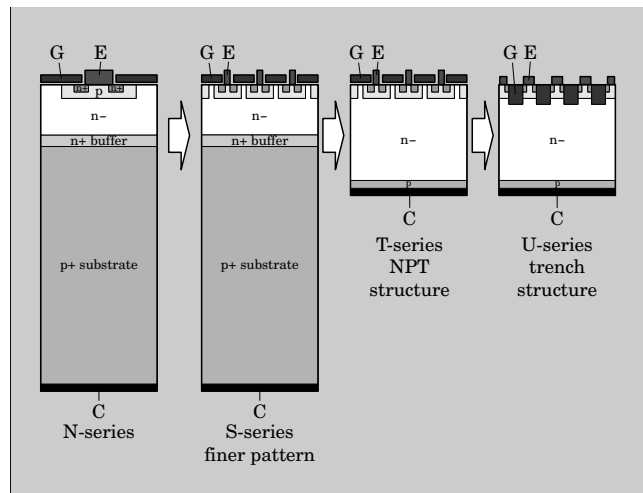
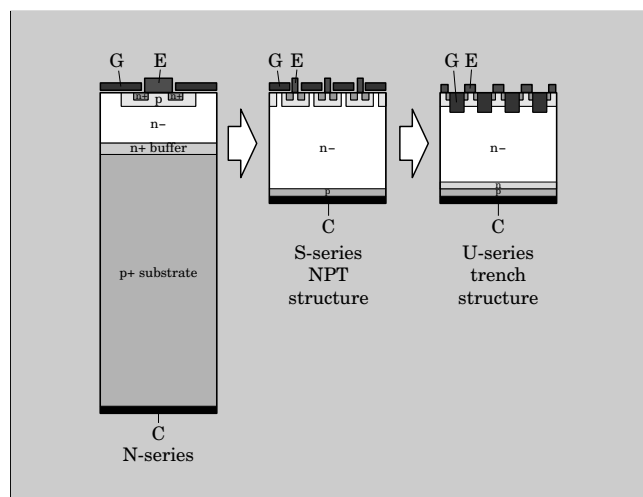


Fig.3 Change in cross-section structure of 1,200 V IGBT chips



tion to improve transistor performance. Improved technology for reducing wafer thickness and the development of process technology for forming FS and P layers at the collector side enabled realization of the 1,200 V- and 1,700 V-fifth-generation IGBT U-series.

Figures 2 and 3 schematically show the cross-section structures of these 600 V and 1,200 V IGBT chips and their transition from generation-to-generation. As can be seen in these figures, recent IGBT chips are significantly thinner than conventional IGBT chips, and advanced technologies such as trench process and FS structure have been incorporated into IGBT chips.

5. Intelligent Power Devices

Fuji Electric has been promoting the development of intelligent power devices in line with the abovementioned development policy. These power devices incorporate driving, self-diagnostic, and computing functions. Fuji Electric's major objective in developing power devices has been to satisfy customers by provid-

ing power devices that solve customer problems. This special issue introduces the newly developed "R-IPM3" series with T-series IGBTs, aiming to reduce power loss, temperature dependence and current concentration, and the "Econo IPM" series, aiming to reduce package size and thickness. Fuji Electric is determined to deliver easy-to-use and low-noise power devices that provide the customer with a comprehensive solution.

In the field of power supplies, the "M-Power1" series has already been commercialized and applied to color televisions, CRT monitors, and other equipment. Recently, Fuji Electric has developed a new system capable of high-speed control even at light loads and proposed the "M-Power2" series which facilitates design of power supplies for LCD (liquid crystal display) monitors, leading to smaller-size, lighter-weight and more efficient power supplies.

In the past, Fuji Electric delivered enhanced-function MOSFETs and intelligent power devices for igniters to the automobile industry. Now, Fuji Electric has developed new vehicle-mounted enhanced-function MOSFETs capable of instantaneously passing a large current at the time of turn-on, such as when switching on a lamp or starting a motor. In addition, protective functions such as overcurrent detection, overcurrent limit and overheat detection are incorporated into the multi-layered fail-safe design.

Through concerted effort with customers, Fuji Electric has been conducting solution-oriented new-product development, concentrating on the fields of general industry, automobile, information and consumer electronics.

6. High-performance Discrete Elements

In 2001, Fuji Electric delivered the power MOSFET "SuperFAP-G" series, which achieved a significant reduction in loss through simultaneously achieving both low R_{on} (on-state resistance) and low Q_{gd} (gate-to-drain charging capacity). In the 450- to 600 V-class, approximately 40 types of power MOSFETs are already being mass-produced. Fuji Electric has recently introduced a series of medium-voltage (100 to 250 V) power MOSFETs for DC-DC converters, and high-voltage (700 to 900 V) power MOSFETs for 200 V AC switching power supplies. In the Super FAP-G series, Fuji Electric's proprietary surface construction mitigated electric field strength on the surface and realized 97% of the theoretical withstand-voltage limits of silicon, thus allowing the use of low resistance wafers. It was indeed a great technological breakthrough.

In the field of switching power supplies, there is demand for improved diodes having lower loss characteristics. In reality, power loss in the secondary output diodes of a switching power supply comprises approxi-

mately half of the total loss. In the past, p-n junction diodes were used for 200 to 300 V power MOSFETs. In order to reduce this loss, Fuji Electric promoted the development of Schottky barrier diodes (SBDs), taking note of their excellent characteristics. A major challenge was optimization of the barrier metal. If the barrier height is too large, forward voltage (V_F) increases, and if barrier height is too small, leakage current (I_L) increases. By overcoming this trade-off relationship, high-voltage SBDs were developed.

7. Conclusion

For the past several years, technological development related to power devices has advanced at a tremendous pace. In a fiercely competitive environment, Fuji Electric has always led in developing power devices with state-of-the-art technology. Fuji Electric has maintained its consistent policy of developing only new products that have the potential to become the leading or only product worldwide in limited market segments.

This special issue introduces Fuji Electric's power devices developed in line with its development policy. The first half of this issue focuses on Fuji Electric's fifth-generation IGBTs (U-series), on which great expectations are placed. Technological innovation related to the U-series, and 600 V, 1,200 V and 1,700 V IGBT modules is also presented in detail.

In addition to IGBTs, this special issue introduces the present status of Fuji Electric's customer-oriented development related to power devices, including intelligent devices in specific fields, dedicated devices for specialized applications and technological innovations for discrete devices.

Fuji Electric is confident that the new products introduced in this special issue will contribute to improved customer satisfaction.

In conclusion, in proclaiming that "**Quality is our message**" and judging itself against that standard, Fuji Electric is determined to provide customers with reliable, high-quality products.

References

- (1) Sawa, K. My Experiences in Developments of Power Electronics. Proceedings of ISPSD'01, 2001, p.461.
- (2) Otsuki, M. et al. Investigation on the Short-circuit Capability of 1,200 V Trench Gate Field-Stop IGBTs. Proceedings of ISPSD'02, 2001, p.281.
- (3) Ohnishi, Y. et al. 24 mohm cm^2 680 V Silicon Super Junction MOSFET. Proceedings of ISPSD'02, 2001, p.241.
- (4) Sugi, A. et al. A 30 V Class Extremely Low On-resistance Meshed Trench Lateral Power MOSFET. Proceedings of ISPSD'02, 2002, p.297.

Technological Innovation for Super-low-loss U-series IGBT Modules

Noriyuki Iwamuro
Tadashi Miyasaka
Yasukazu Seki

1. Introduction

The IGBT (insulated gate bipolar transistor) originated in the first half of 1980s as a power device having both the high impedance characteristic of a MOSFET (metal oxide semiconductor field effect transistor) and the low on-state voltage characteristic of a bipolar transistor. Since the advent of the first generation IGBT in the latter half of 1980s, IGBTs have played an important role in power electronics technology in the fields of industry, information, traffic control, etc. The IGBT has attracted attention year after year because of its advantageous voltage/current ratings and excellent switching capability which is superior to that of the bipolar transistor. Accordingly, there is strong demand for the development of lower power loss IGBTs. Through the adoption of finer surface cell construction and the resultant high-performance technical innovations, first, second and third generation IGBTs have been developed, subsequently enabling smaller size and higher performance equipment. In recent years, the performance of IGBT modules has been improved dramatically. This paper describes the design concept and characteristics of the super-low-loss U-series IGBT module developed by Fuji Electric and introduces the IGBT module technological innovations achieved by Fuji Electric.

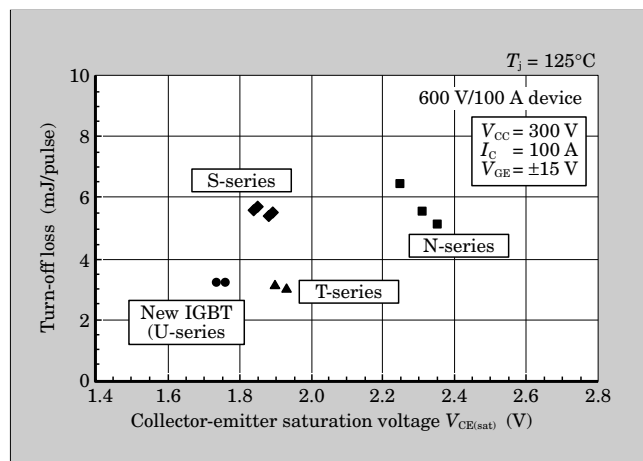
2. Development of Super-low-loss IGBT Chips

Fuji Electric started producing IGBTs in 1988, and has been supplying them to the market ever since. Based on the design concept to increase injection efficiency of the wide base pnp transistor and decrease the transportation factor by lifetime control, we improved the characteristics of PT (punch through) type IGBTs by adopting fine surface cell construction to increase the supply of electron current from the MOSFET portion. First, second and third generation (N-series) IGBTs were developed in 1988, 1990 and 1994, respectively, based on this technology. Thereafter, to improve the performance further, we developed the NPT (non-punch through) type IGBT (NPT-IGBT) based on the design concept to decrease injection

efficiency of the above pnp transistor and to increase the transportation factor without using lifetime control. In developing the NPT-IGBT, we were able to improve its characteristics by adopting a new thin wafer process technology in which the devices are fabricated from a wafer shaved down to a thickness of almost 100 μm . Based on this technology, the S-series (1,200 V type) and T-series (600 V type) IGBTs were developed in 1999 and 2001, respectively.

The newly developed super-low-loss IGBT chip (U-IGBT chip) is a power semiconductor, featuring improved characteristics enabled by the adoption of thin wafer process technology developed for NPT-IGBT chip and trench gate technology and which will realize fine surface cell construction. Figure 1 compares the saturation voltage turn-off loss trade-off for 600 V type IGBT chips of several generations. From this figure, it is clear that a great improvement has been achieved by trench gate structure and thin wafer NPT construction. To improve thin wafer NPT technology, we developed thin wafer FS (field stop) technology⁽¹⁾ and applied it to 1,200 V and 1,700 V IGBT chips. As shown on Fig. 2, saturation voltage turn-off loss characteristic was improved dramatically. Because the U-IGBT chip adopts the design concept of reduced injection efficiency of the pnp transistor and increased transportation factor without lifetime control, the

Fig.1 600 V IGBT trade-off comparison



saturation voltage has a positive temperature coefficient as shown in Fig. 3. Therefore, this device is suitable for high rated current applications.

In designing IGBTs, it is already known that saturation voltage can be reduced by adopting a fine surface cell construction, such as a trench gate structure. But, on the contrary, during abnormal conditions such as a load short circuit, a high current may flow into the device. Therefore, the device could be damaged. A solution to this problem was an important

Fig.2 1,200 V & 1,700 V IGBT trade-off comparison

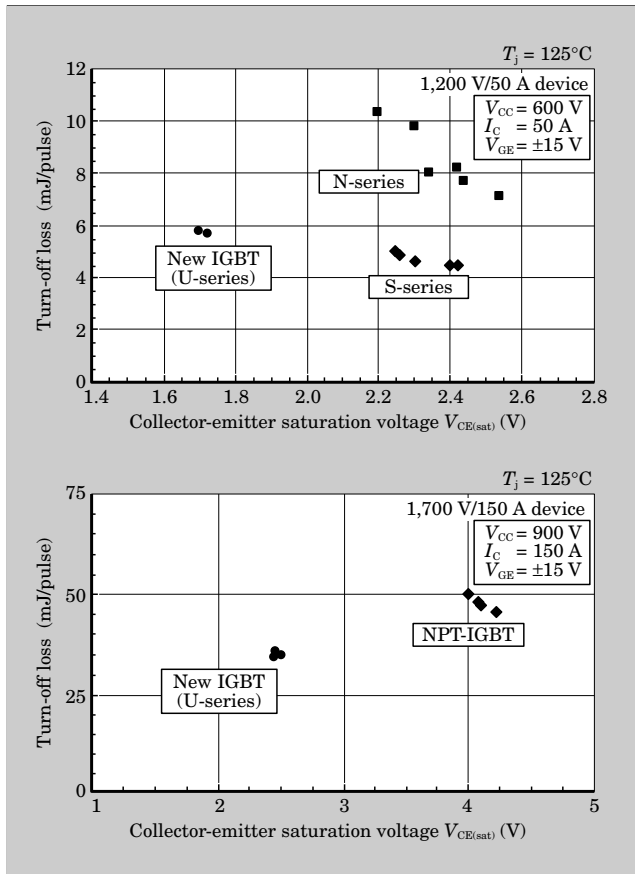
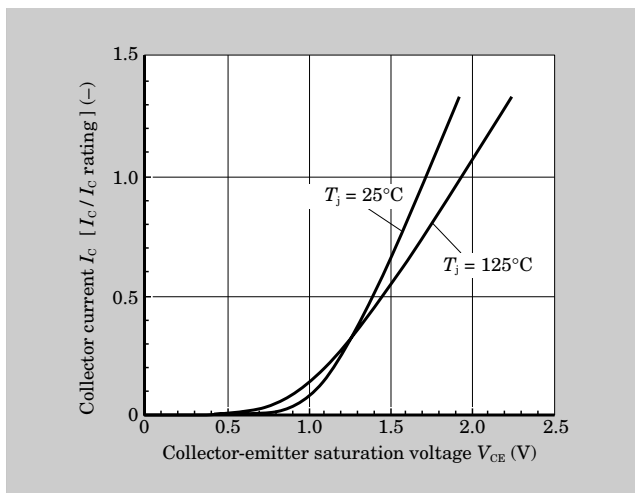


Fig.3 U-IGBT output characteristics (1,200 V device)



theme of the development. In the newly developed U-IGBT chip, the current during a load short circuit is suppressed by an optimized trench gate structure that does not sacrifice the on-voltage, and as a result, the endurance is improved. Figure 4 shows the load short circuit waveform of a 1,200 V / 450 A U-IGBT module. The current during a load short circuit is limited to within about 5 times the rated current. Even at 125°C, the device can withstand this current for more than 10 μs.

3. Features of New FWD Chips

The new FWD (free wheeling diode) has a soft reverse recovery characteristic that is achieved by controlling the injection of minority carriers from the anode layer. As in the case of the IGBT, the new FWD is designed with optimized lifetime control such that on-state voltage has a positive temperature coefficient. Therefore, this device is suitable for high rated current applications. Through the adoption of the new FWD, peak current during turn-on of the IGBT was reduced

Fig.4 U-IGBT (1,200 V / 450 A) waveforms during load short circuit

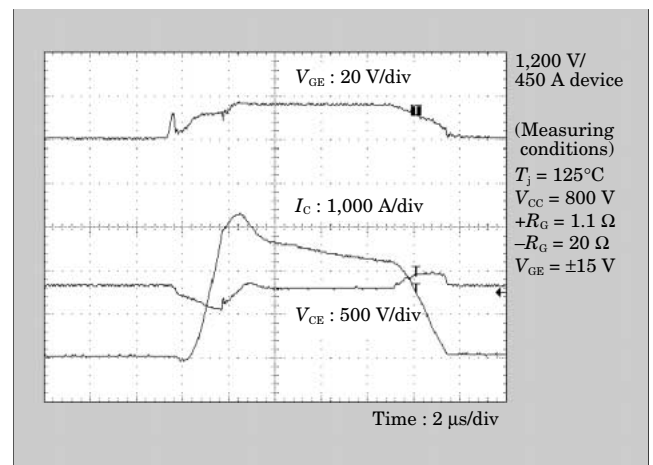
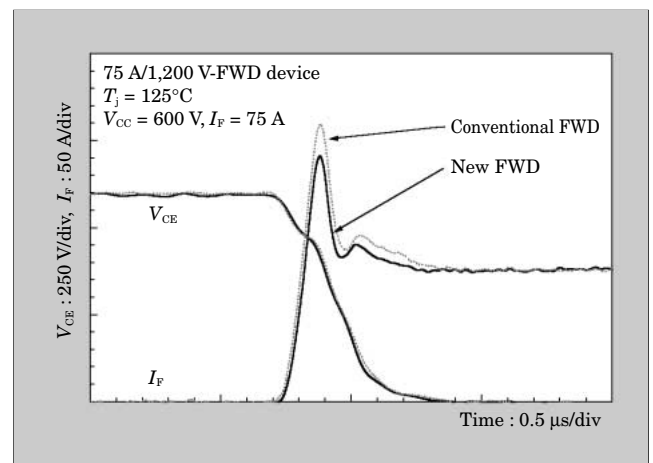


Fig.5 Comparison of IGBT turn-on waveforms for U-FWD and conventional FWD



as shown on Fig. 5. As a result, turn-on power loss was reduced.

4. Thermal Characteristics of U-IGBTs when applied to Inverters

IGBT modules are widely used in general-purpose inverters. Further improvement in performance and reliability is requested to enhance the cost-performance attribute. Figure 6 shows the correlation between chip size and power loss when an IGBT is used in an inverter. For example, the power loss of a 30 kW inverter using a new 1,200 V / 150 A device at the rated load condition can be reduced by about 30 % compared with the power loss when using conventional devices with the same chip size. Dependency of the chip size on the power loss is relatively low. This suggests that the chip size could be shrunk by about 20 % assuming the same power loss. By adopting the above mentioned chip technology, the IGBT output

Fig.6 Comparison of power loss and chip size of IGBT

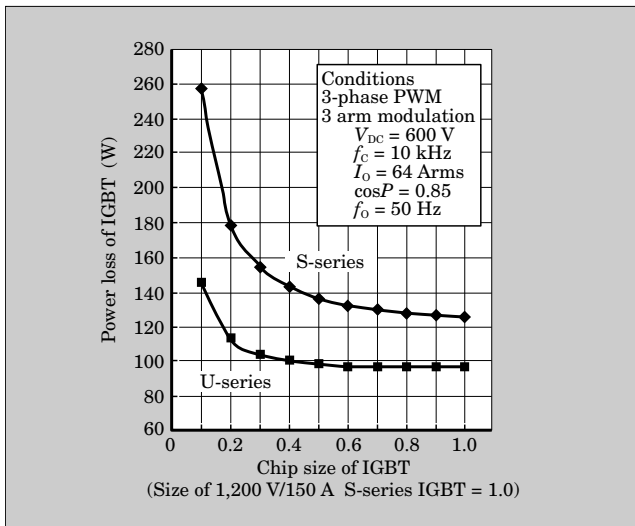
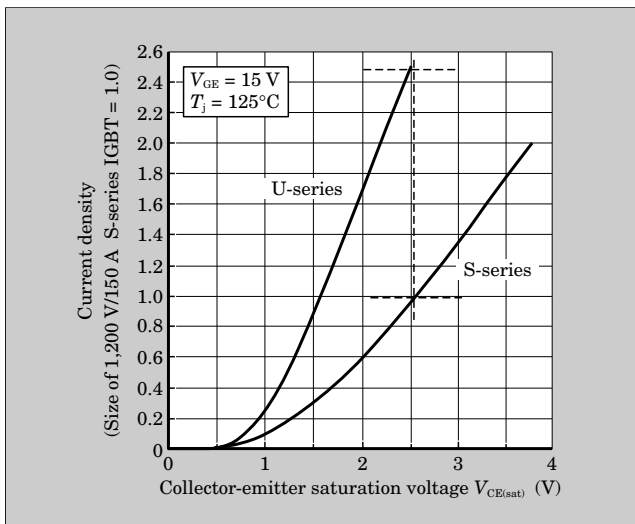


Fig.7 Comparison of output characteristics of IGBT



characteristic was improved as shown on Fig. 7. This improvement was realized because of the fact that the saturation voltage will not be increased by the increase in current density.

As shown on Fig. 8, the thermal resistance ($R_{th(j-c)}$) is inversely proportional to the chip size. If we calculate the chip temperature rise (ΔT_{j-c}) simply by the formula $\Delta T_{j-c} = \text{power loss} \times R_{th}$, the temperature rise can be increased rapidly by shrinking the chip size. This may cause problems with the reliability of power cycle capability.

4.1 Temperature rise of an IGBT chip (including the cooling system)

The temperature rise of an IGBT chip is dependent on the cooling system, including the radiators. In the

Fig.8 Comparison of ΔT_{j-c} and chip size of IGBT

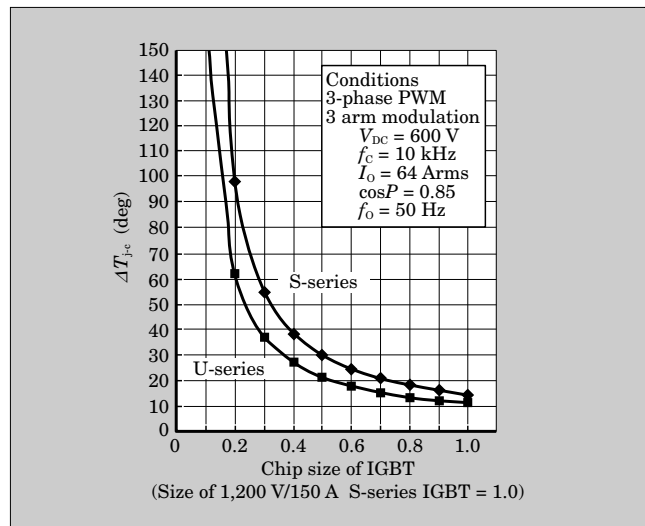


Fig.9 FEM analysis results of chip temperature rise of IGBT

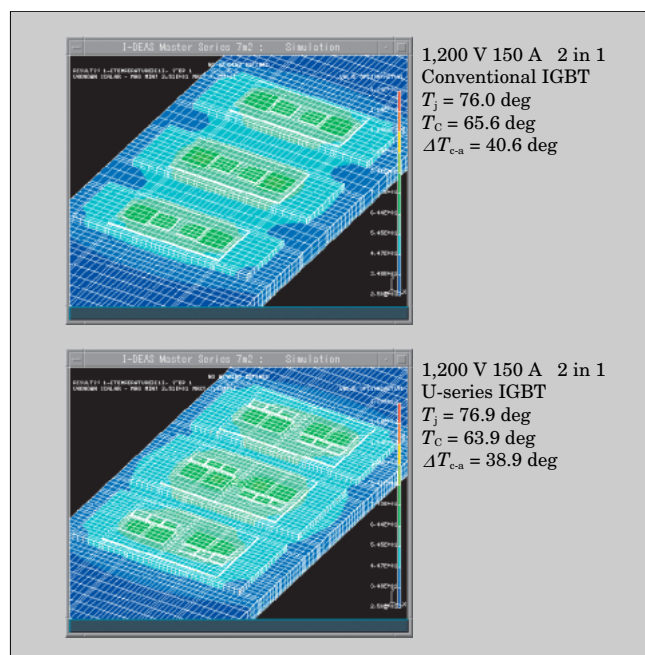
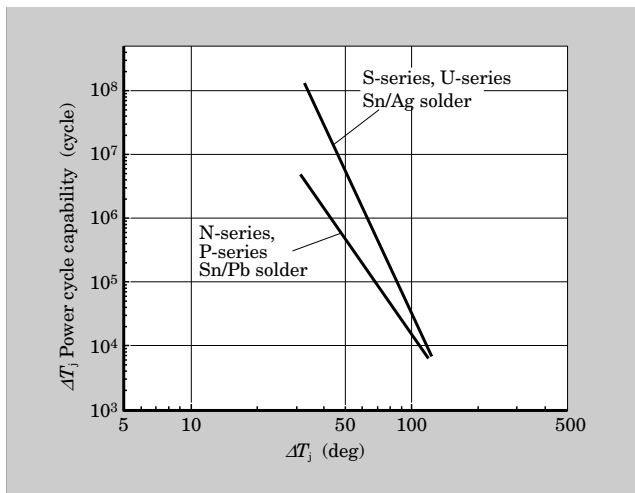


Fig.10 Improvement of power cycle capability



past, the temperature rise of an IGBT chip was calculated assuming a constant cooling fin temperature and the chip temperature rise was calculated as the summation of the constant cooling fin temperature and ΔT_{j-c} .

Figure 9 shows the results of calculating the temperature rise of an IGBT chip, including the cooling system, by the finite elements method (FEM). Results of three-dimension model analysis suggest the following possibilities for controlling chip temperature rise.

- (1) Sideways thermal spreading of the cooling system mounting base
- (2) Reduction of mutual interference by the optimizing chip intervals
- (3) Optimization of module arrangement

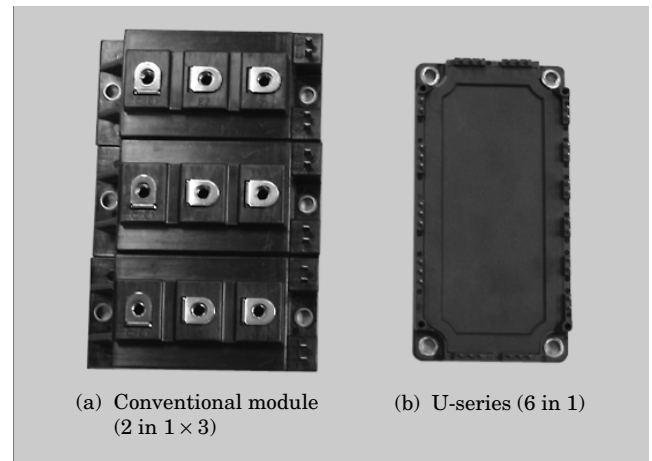
With this analysis method, the temperature rise, which is important for verifying the reliability, can be calculated easily and precisely.

4.2 Improvement of power cycle capability

Based on the analysis of test devices subject to power cycles in an IGBT module, we verified that the power cycle capability is dependent on the combined total life of solder and bonding wires at the bottom of the chip. We reported a new technique for changing to a high elasticity tin solder on the chip bottom to extend the life⁽²⁾.

We applied this technology to the U-series. As shown on Fig. 10, the power cycle capability of the U-series is more than 10 times that of the conventional series at $\Delta 40$ deg. In other words, to keep the same power cycle capability, the allowable temperature rise

Fig.11 Comparison of appearance of U-IGBT and conventional module



can be increased to up to 60 deg as contrasted with the usual allowable temperature rise of 40 deg.

Figure 11 compares the modules of the conventional 1,200 V / 150 A device and those of the U-series device. The new technology achieves a space savings of 40 % (area of the base).

5. Conclusion

An overview of the chip and packaging technology of the new super-low-loss U-series IGBT module was presented above. The U-series IGBT chip, with its almost ideally shaped IGBT due to the combination of trench gate structure and thin wafer technology, contributes to the loss reduction and miniaturization of equipment. To make maximum use of an IGBT module, it is necessary to fully understand the worst operating condition and to select the most appropriate device for that condition, considering the thermal characteristics of the cooling device. Fuji Electric has developed device technology for this purpose and will strive to further enhance this new technology and apply it to equipment.

References

- (1) Laska, T. et al. The Field Stop IGBT (FS-IGBT) - A New Power Device Concept with a Great Improvement Potential. Proceedings of the 12th ISPSD. 2000, p.355-358.
- (2) Morozumi, A. et al. Reliability of Power Cycling for IGBT Power Semiconductor Module. Conf. Rec. IEEE Ind. Appl. Conf. 36th. 2001, p.1912-1918.

T-series and U-series IGBT Modules (600 V)

Seiji Momota
Syuuji Miyashita
Hiroki Wakimoto

1. Introduction

The IGBT (insulated gate bipolar transistor) module is the most popular power device in power electronics fields such as motor control applications. The reason for the IGBT's popularity is the market values of its excellent reliability due to reduction of generated loss and increase of withstand capability, etc., in addition to the fact that it can be easily driven. The 600 V IGBT modules play an especially important role as key devices in a wide market area including the Japanese domestic market where 220 V industrial power supplies are used and overseas such as in Europe where 200 V public power supplies are used as general-purpose power supplies.

Under these circumstances, Fuji Electric has also been developing a 600 V IGBT module product series, and has continued to improve their characteristics ever since first developing the series in 1988. In 2001, the development of thin wafer processing technology enabled NPT (non-punch through) structure to be applied to 600 V devices. This made possible the development of T-series IGBTs, having low switching loss and being especially suitable for high frequency applications.

While development of NPT technology mainly involved by development of the structure at the back of the chip, improvements of the chip's front structure have also been implemented since 2002. By applying trench-gate-structure, increase in channel density and elimination of the unnecessary voltage-drop component was achieved, thereby enabling the reduction of on-state loss. This made the development of U-series IGBTs successful, as the device having the smallest loss among products of its class, and at present, we are in the process of producing various rated current series and sample modules.

For the FWD (free wheeling diode) packed in IGBT modules, enhanced soft-recovery characteristics as well as decreased loss is demanded. These demands are not only for the sake of preventing equipment malfunction, but also to preventing possible ill effects of noise emission on the surrounding equipment and on the human body. To satisfy these requirements, FWDs having a new structure were developed and adopted

for the above new IGBT modules. This paper presents these device techniques and the product series.

2. T-series IGBT Modules

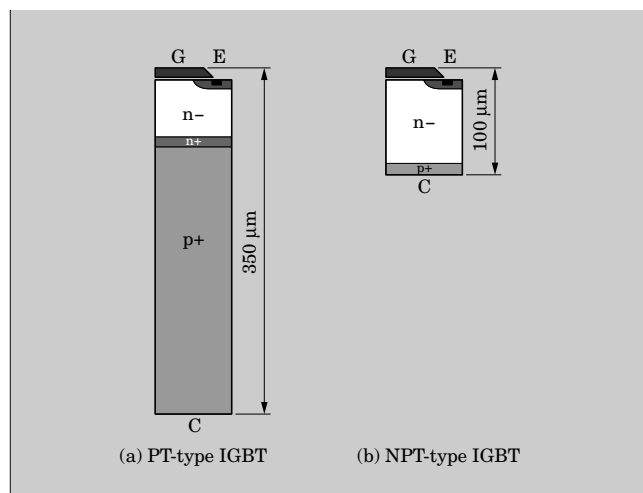
2.1 Features and challenges of T-series IGBT modules

The cell structure of an NPT-type IGBT and the unit cell of PT (punch-through)-type device are shown in Fig. 1. Their features are as follows:

- (1) Since injection from the collector-side can be suppressed, lifetime control is unnecessary and the switching loss does not increase even at a high temperature.
- (2) Because the temperature dependence of output characteristics is positive (the saturation voltage increases at higher temperatures), these devices are well suited for parallel applications.
- (3) Withstand capability including load short-circuit capacity are higher than those of a PT-type device.
- (4) Use of an FZ (floating zone) wafer makes the price cheap and the reliability high owing to its low crystal defects.

The challenge is to establish a thin wafer processing technique. It is important for NPT-type devices to suppress saturation voltage while maintaining the collector-emitter (CE) forward blocking voltage. This

Fig.1 Comparison of unit cell structures



requires keeping the depletion layer end thick enough so there is no punch-through even when the maximum CE voltage is applied. The optimal thickness is thinner for devices having lower CE forward blocking voltage, making their manufacturing even more difficult.

2.2 Fuji Electric approach to NPT devices

Fuji Electric has been involved in developing NPT technology earlier on as shown in Fig. 2, and is working to extend the application of this technology to more challenging devices having lower forward blocking voltage, making their manufacturing even more difficult.

Although the optimal thickness for 600 V-NPT IGBTs application is said to be about 100 μm based upon various investigations, Fuji Electric has made it possible to set the thickness lower than that of the other companies through improved precision of back-grinding process technology. This was effective in reducing saturation voltage and turn-on loss, which were factors contributing to generated loss or inverter loss.

2.3 Characteristics of T-series IGBTs

An overview of the characteristics of T-series IGBTs is presented below. Figure 3 compares V_{CES} waveforms, namely the CE-forward blocking voltages, in which the forward blocking voltage of the NPT

Fig.2 Changes in Fuji Electric's application of NPT technology

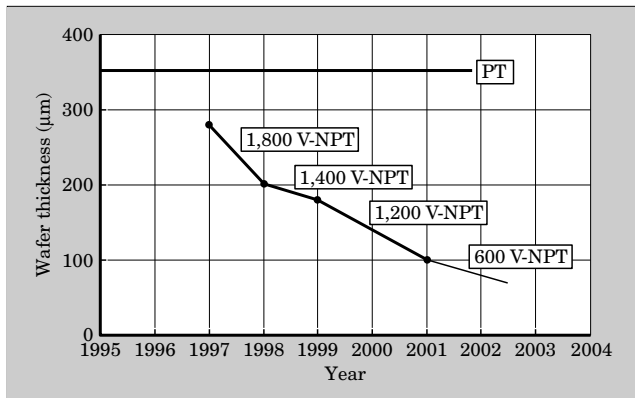
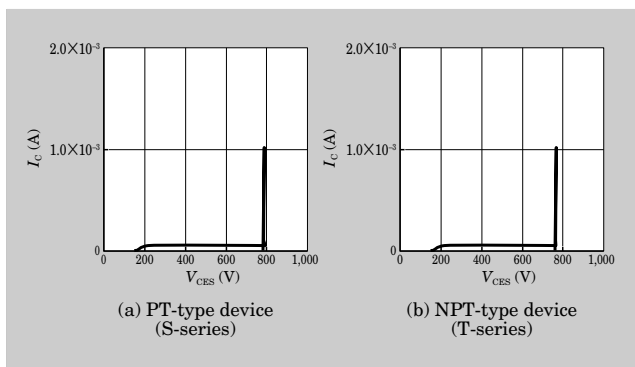


Fig.3 Comparison of V_{CES} waveforms of PT-type device and NPT-type device



device is about 800 V, similar to that of the PT device, and higher than the maximum rated voltage of 600 V.

Figure 4 shows a comparison of turn-off waveforms. In PT-type devices, which are injected more from the collector side, lifetime control is implemented to promote the recombination of carriers at the time of turn-off. However, because this effect decreases as the temperature increases, the loss tends to increase caused by the increase of tail current. For NPT-type devices, on the other hand, no lifetime control is applied and therefore these temperature dependence do not exist, resulting in no change in the turn-off waveform and no increase in turn-off loss.

The load short-circuit waveforms are shown in Fig. 5. When the load is short-circuited, devices breakdown due to the temperature rise resulting from the generated energy loss.

However, the NPT-type device, having a thick n-drift layer, can support the voltage with its wide n-drift layer, and the temperature rise which causes breakdown can be suppressed, resulting in high short-circuit withstand capability. Compared with the withstand capability of 15 μs of a PT-type device, the NPT-type device has a real capability of 22 μs , which is

Fig. 4 Comparison of turn-off waveforms

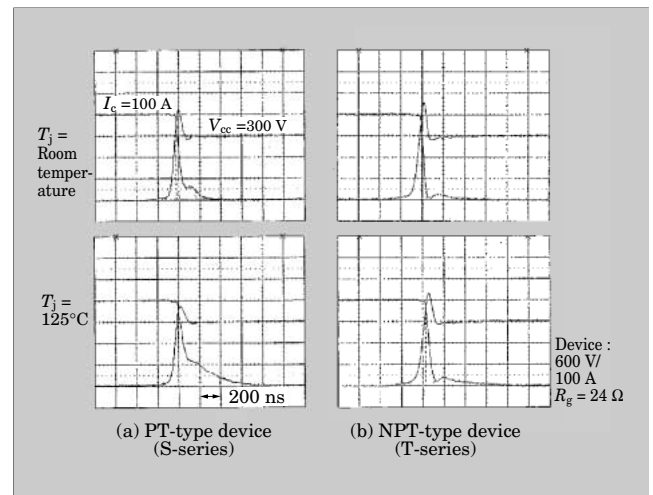
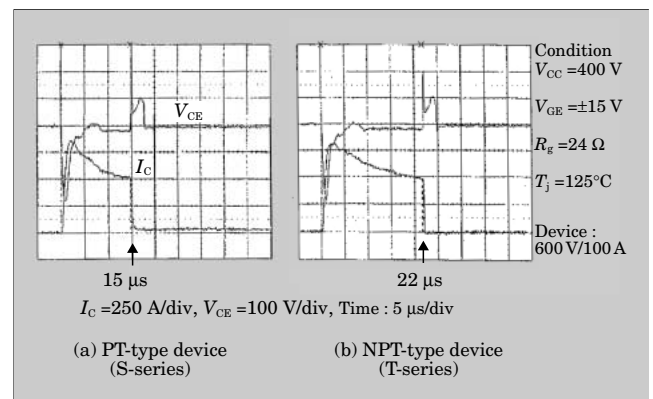


Fig.5 Comparison of load short-circuit waveforms



sufficiently above the usually required 10 μs .

3. U-series IGBT

3.1 Chip front cell structure of U-series IGBT

Improvements were applied to the emitter side structure of the T-series IGBT chip, having already had its back structure improved, for the purpose of further collector side performance enhancement. Fuji Electric is producing trench-gate type power MOSFETs (metal oxide semiconductor field effect transistors), to which design and process technologies have been applied, to ensure sufficient reliability to permit installation in motor vehicles. The U-series IGBT is the result of applying these techniques to IGBTs. Figure 6 compares this cell structure with that of the T-series planar type.

The trench type IGBT allows drastic increase in cell density, resulting in suppression of the voltage drop at the channel part to a minimum. Since the

Fig.6 Comparison of planar and trench type cell structures

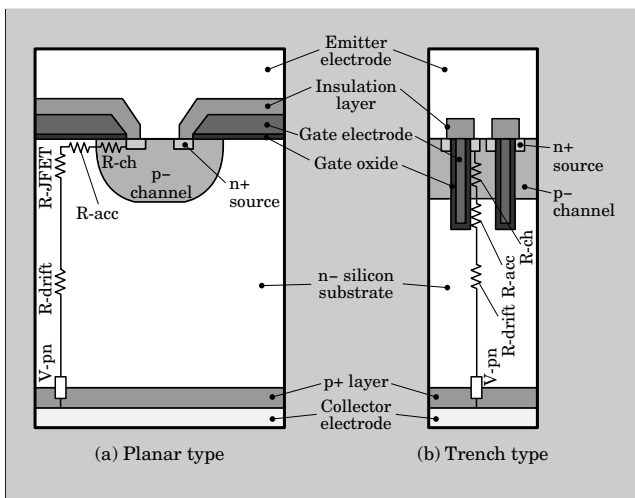
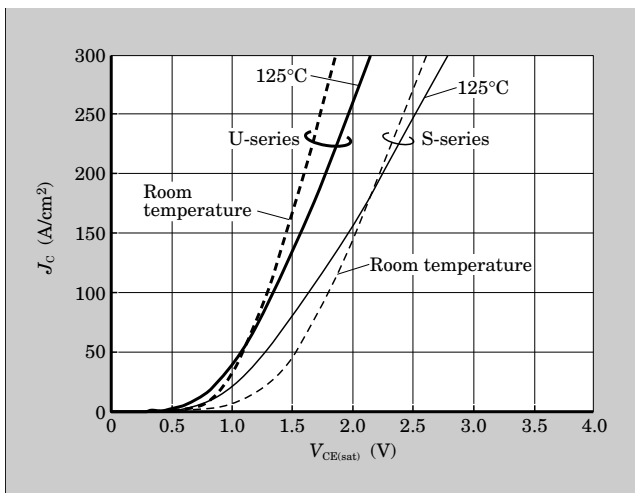


Fig.7 Comparison of saturation voltages between collector and emitter, and of collector current output characteristics



distinctive J_{FET} region, sandwiched between channels of the planar type device, does not exist in the trench type device, the voltage drop at this region can be completely eliminated. However, a standard cell design cannot be applied to power MOSFETs having a low blocking voltage below 100 V, and instead, a new cell pitch and trench depth appropriate for 600 V IGBTs should be applied. The optimal values for U-series IGBTs were investigated using simulations and experiments, and then applied to the cell design.

3.2 Characteristics of U-series IGBTs

Characteristics of U-series IGBTs, designed based upon the aforementioned techniques, are described below. First, the output characteristics of saturation voltage between collector and emitter ($V_{\text{CE(sat)}}$) and collector current are shown in Fig. 7.

$V_{\text{CE(sat)}}$ for a current density of 185 A/cm² (at $T_j = 125^\circ\text{C}$) was significantly reduced from 2.15 V down to 1.70 V. The intersects of the output characteristics at room temperature and at high temperature lies in the lower current area, and the temperature dependence

Fig.8 Comparison of loss generation of various devices

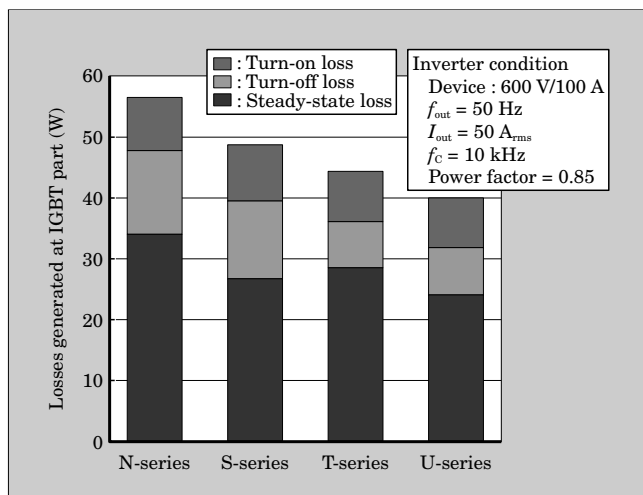


Fig.9 FWD output characteristics

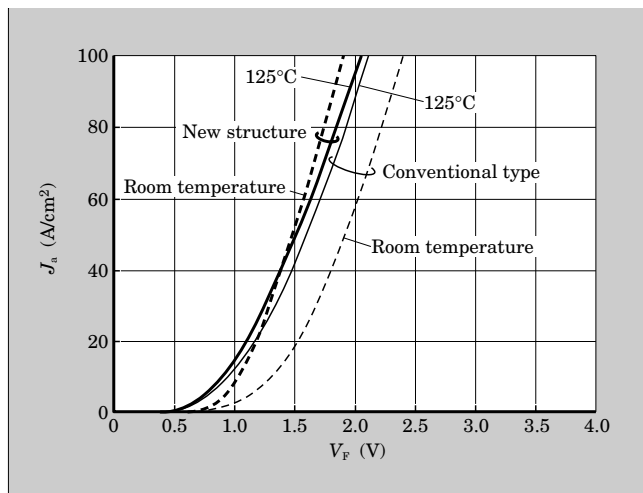
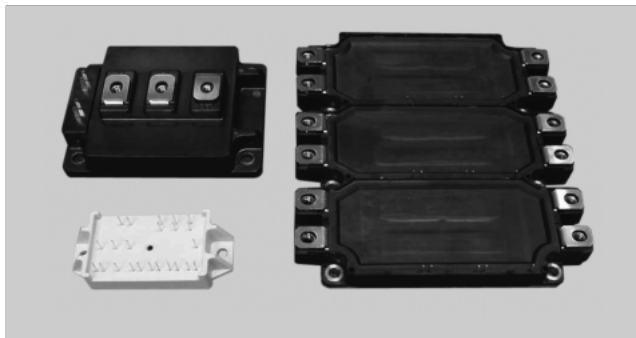


Table 1 U-series IGBTs

Package	Rated current	Model	Product release date
Small capacity PIM	8 A	7MBR8UE060	April 2003
	10 A	7MBR10UE060	
	15 A	7MBR15UE060	
	20 A	7MBR20UE060	
	30 A	7MBR30UE060	
EP2	20 A	7MBR20UA060	
	30 A	7MBR30UA060	
	50 A	7MBR50UA060	
EP3	50 A	7MBR50UB060	
	75 A	7MBR75UB060	
	100 A	7MBR100UB060	
HEP2	20 A	7MBR20UC060	
	30 A	7MBR30UC060	
	50 A	7MBR50UC060	
HEP3	75 A	7MBR75UD060	
	100 A	7MBR100UD060	
7in1 (M631 or M621)	100 A	7MBI100UD-060	
	150 A	7MBI150UD-060	
	200 A	7MBI200UD-060	
	300 A	7MBI300UD-060	
M232	150 A	2MBI150UA-060	
	200 A	2MBI200UA-060	
M233	300 A	2MBI300UB-060	
	400 A	2MBI400UB-060	
M238	600 A	2MBI600UE-060	
M629	400 A	6MBI400U-060	
	600 A	6MBI600U-060	

Fig.10 Typical package of U-series IGBT



in the normal-use area are positive. These positive temperature dependence can reduce the behavior unbalance between devices when using large capacity modules parallel, and can elongate the lifespan of the products. These characteristics result from the facts that lifetime control is not implemented and that the n-drift layer is thick, which are common features of the T-series and U-series.

Figure 8 compares the calculated results of loss generation for various devices when the current density is kept at the same value. Application of an NPT-

Table 2 Major ratings of 2MBI400UB-060 (tentative)

(a) Absolute max. ratings ($T_c = 25^\circ\text{C}$ unless specified otherwise)

Item	Symbol	Condition	Max. rating	Unit
Collector-emitter voltage	V_{CES}		600	V
Gate-emitter voltage	V_{GES}		± 20	V
Collector current	I_C	Continuous	400	A
	$I_{C\ pulse}$	1 ms	800	
	$-I_C$		400	
	$-I_{C\ pulse}$	1 ms	800	
Maximum power dissipation	P_C	1 device	1,135	W
Junction temperature	T_j		150	$^\circ\text{C}$
Storage temperature	T_{stg}		-40 to +125	$^\circ\text{C}$
Isolation voltage (package)	V_{iso}	AC : 1 min	2,500	V
Screw fastening torque	Mounting		3.5	Nm
	Terminals		3.5	

(b) Electrical characteristics ($T_c = 25^\circ\text{C}$ unless specified otherwise)

Item	Symbol	Condition	Characteristics			Unit	
			min.	typ.	max.		
Zero gate voltage collector current	I_{CES}	$V_{GE} = 0\text{ V}$, $V_{CE} = 600\text{ V}$	-	-	2.0	mA	
Gate-emitter leakage current	I_{GES}	$V_{CE} = 0\text{ V}$, $V_{GE} = \pm 20\text{ V}$	-	-	0.4	μA	
Gate-emitter threshold voltage	$V_{GE(th)}$	$V_{CE} = 20\text{ V}$, $I_C = 400\text{ mA}$	-	6.0	-	V	
Collector-emitter saturation voltage	$V_{CE(sat)}$ (Terminal)	$V_{GE} = 15\text{ V}$, $I_C = 400\text{ A}$	$T_j = 25^\circ\text{C}$	-	1.8	-	V
			$T_j = 125^\circ\text{C}$	-	1.9	-	
	$V_{CE(sat)}$ (Chip)	$T_j = 25^\circ\text{C}$	-	1.6	-		
		$T_j = 125^\circ\text{C}$	-	1.7	-		
Input capacitance	C_{ies}	$V_{GE} = 0\text{ V}$, $V_{CE} = 10\text{ V}$ $f = 1\text{ MHz}$	-	40	-	nF	
Turn-on time	t_{on}	$V_{CC} = 600\text{ V}$, $I_C = 400\text{ A}$, $V_{GE} = \pm 15\text{ V}$, $R_g = 0.5\ \Omega$	-	-	1.2	μs	
	t_r		-	-	0.6		
Turn-off time	t_{off}		-	-	1.0		
	t_f		-	-	0.35		
Diode forward voltage	V_F (Terminal)	$I_F = 400\text{ A}$	$T_j = 25^\circ\text{C}$	-	1.8	-	V
			$T_j = 125^\circ\text{C}$	-	1.7	-	
	V_F (Chip)		$T_j = 25^\circ\text{C}$	-	1.6	-	
			$T_j = 125^\circ\text{C}$	-	1.5	-	
Reverse recovery time	t_{rr}	$I_F = 150\text{ A}$	-	-	0.3	μs	

(c) Thermal resistance characteristics

Item	Symbol	Condition	Characteristics			Unit
			min.	typ.	max.	
Thermal resistance of device (1 device)	$R_{th(j-c)}$	IGBT	-	-	0.11	$^\circ\text{C/W}$
		FWD	-	-	0.18	
Case to fin thermal resistance	$R_{th(c-f)}$		-	0.025	-	

type structure reduced the turn-off loss drastically in the T-series module, resulting in an approximate 10 %

reduction in total IGBT loss, compared with the S-series. For U-series IGBT modules, in which on-state energy loss has been decreased due to a reduction of $V_{CE(sat)}$, an additional 10 % reduction of loss has been realized.

4. Improvement of FWD

An FWD is packed into an IGBT module together with an IGBT, and the FWD is required to have soft recovery characteristics and reduced levels of generated loss. The improvements include optimization of wafer specifications, injection control from the anode at the chip's front structure and implementation of optimal lifetime control. Fuji Electric has developed FWDs with a revised new design. The output characteristics are shown in Fig. 9. As a result, the forward voltage (V_F) has been reduced and positive temperature dependence have been realized. Because carrier injection is suppressed, the peak current at reverse recovery has been reduced, loss generation has been reduced, and soft-recovery characteristics have been

achieved. These improvements led to the realization of an FWD having low generated loss and low noise, and enabled its application to the U-series module.

5. Introduction of Product Series

Details of the U-series IGBT product lineup are as follows. The U-series IGBT product lineup and product release date are shown in Table 1, and the external view of a typical package is shown in Fig. 10. The major ratings and characteristics of U-series IGBTs are shown in Table 2.

6. Conclusion

The T-series and U-series of IGBTs for 600 V-NPT modules were introduced. Fuji Electric will continue to advance the high performance of these modules by developing specific technology for IGBTs and by incorporating technologies of other types of semiconductors, and will strive to contribute to the overall development of power electronics.



U-series IGBT Modules (1,200 V)

Yuichi Onozawa
Shinichi Yoshiwatari
Masahito Otsuki

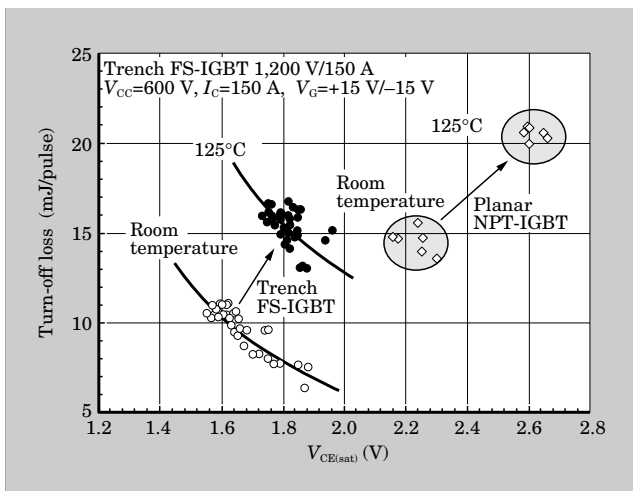
1. Introduction

Power conversion equipment such as general-use inverters and uninterruptible power supplies (UPSs) is continuously challenged by demands for higher efficiency, smaller size, lower cost and lower noise. Accordingly, power-converting elements for inverter circuits are also required to have higher performance and lower cost. At present, IGBTs (insulated gate bipolar transistors) are the main power-converting elements used because of their low loss and easy drive circuit implementation. After commercializing the IGBT in 1988, Fuji Electric has made efforts to improve the IGBT in pursuit of lower loss and lower cost. This paper introduces fifth generation IGBT modules (U-series), and focuses on the 1,200 V series used mainly in 400 V AC power lines overseas. Adoption of a trench gate structure and a field stop (FS) structure has resulted in a large improvement in the trade-off characteristics of fifth generation IGBTs compared with those of the fourth generation IGBT (S-series).

2. Features of the New IGBTs

Figure 1 shows the trade-off relation of the saturation

Fig.1 Trade-off between $V_{CE(sat)}$ and turn-off loss



tion voltage between the collector and emitter ($V_{CE(sat)}$) and the turn-off loss of the newly developed IGBT (trench FS-IGBT). From this figure, it can be seen that the trade-off of the 1,200 V U-series IGBT is dramatically improved compared to that of the former generation S-series IGBT [planar NPT (non punch through) -IGBT]. This dramatic improvement in characteristics has been achieved through adopting a field stop structure, evolved from an advanced NPT configuration, and a trench gate structure, acquired during development of MOSFETs (metal oxide semiconductor field effect transistors). Each of these structures is described below.

2.1 Field stop structure

Figure 2 shows output characteristics and Fig. 3 shows comparison of cross section of unit cells of a planar NPT-IGBT and a planar FS-IGBT. An NPT-IGBT requires a thick drift layer so that the depletion layer does not contact the collector side during turn-off. The FS-IGBT does not, however, require such a thick drift layer as the NPT because a field stop layer to stop the depletion layer has been fabricated in the FS-IGBT and accordingly $V_{CE(sat)}$ can be lowered for the FS-IGBT. Furthermore, the FS-IGBT has fewer excess carriers because of its thinner drift layer. Moreover,

Fig.2 Output characteristics

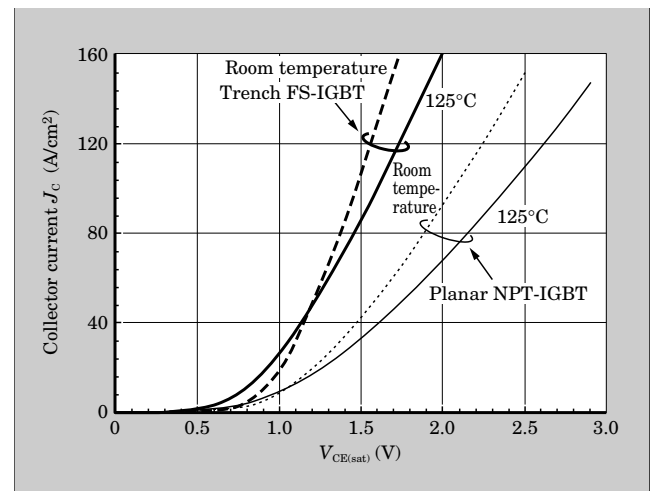


Fig.3 Comparison of cross sections of unit cells of a planar NPT-IGBT and a planar FS-IGBT

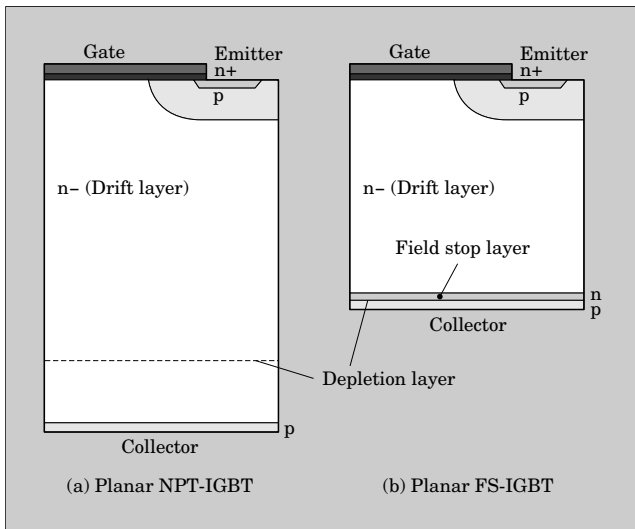
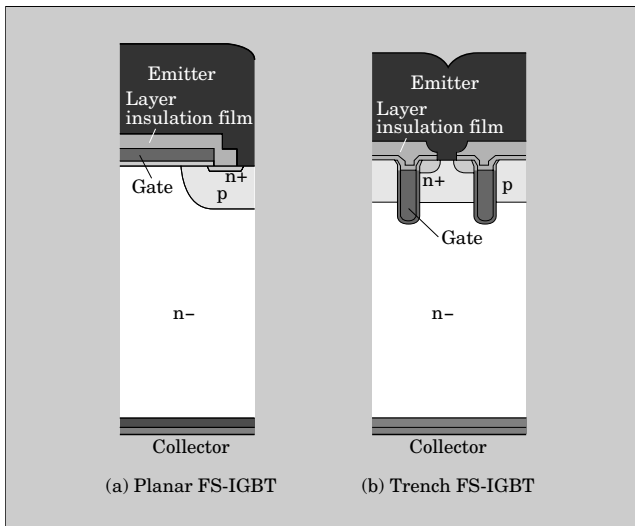


Fig.4 Comparison of cross sections of IGBT unit cells



the FS-IGBT can achieve reduced turn-off loss because the remaining width of its neutral region is small when its depletion layer is completely extended.

2.2 Trench gate structure

Figure 4 shows a cross section of a trench FS-IGBT. By adopting a trench gate structure, channel density can be increased and $V_{CE(sat)}$ can be significantly lowered because resistance in the J_{FET} part, which was problematic for planar IGBTs when cell density increased, can be reduced to zero.

On the other hand, the high channel density of the trench IGBT causes a problem of low short-circuit capacity. However, the trench gate structure optimizes the total channel length to realize high short-circuit capacity without sacrificing $V_{CE(sat)}$ (Fig. 5).

Fig.5 Short-circuit waveforms

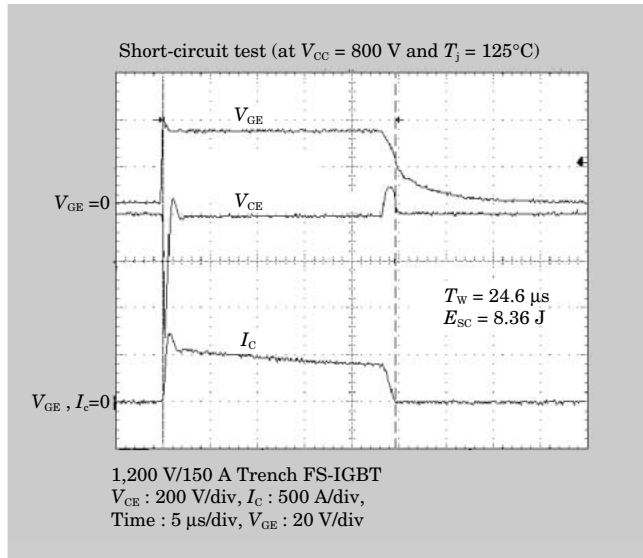


Fig.6 Comparison of turn-on waveforms

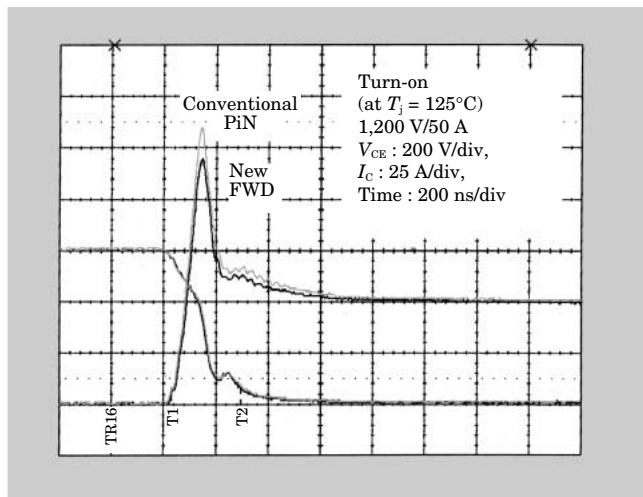


Fig.7 Comparison of FWD output characteristics

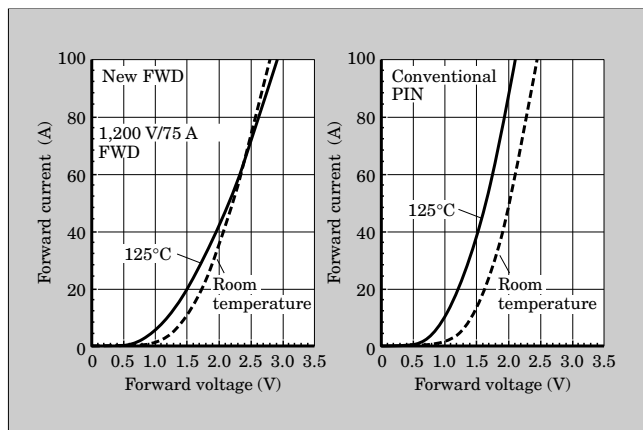


Table 1 Characteristics of the 1,200 V U-series IGBT modules
(a) Absolute maximum ratings (at $T_c = 25^\circ\text{C}$ unless otherwise specified)

Item	Symbol	Condition	Max. rating	Unit	
Collector-emitter voltage	V_{CES}		1,200	V	
Gate-emitter voltage	V_{GES}		± 20	V	
Collector current	I_C	Continuous	$T_j = 25^\circ\text{C}$	150	A
			$T_j = 80^\circ\text{C}$	100	
	$I_{C\text{ pulse}}$	1 ms	$T_j = 25^\circ\text{C}$	300	
			$T_j = 80^\circ\text{C}$	200	
			$-I_C$	100	
$-I_{C\text{ pulse}}$	1 ms	200			
Maximum loss	P_C	1 device	600	W	
Junction temperature	T_j		150	$^\circ\text{C}$	
Preserving temperature	T_{stg}		-40 to +125	$^\circ\text{C}$	
Isolation voltage (package)	V_{iso}	AC : 1 min	2,500	V	
Screw fastening torque	Mounting		3.5	Nm	
	Terminals		3.5		

(b) Electrical characteristics (at $T_c = 25^\circ\text{C}$ unless otherwise specified)

Item	Symbol	Condition	Characteristics			Unit	
			min.	typ.	max.		
Collector-emitter leakage current	I_{CES}	$V_{GE} = 0\text{ V}$, $V_{CE} = 1,200\text{ V}$	-	-	1.0	mA	
Gate-emitter leakage current	I_{GES}	$V_{CE} = 0\text{ V}$, $V_{GE} = \pm 20\text{ V}$	-	-	0.2	μA	
Gate-emitter threshold voltage	$V_{GE(th)}$	$V_{CE} = 20\text{ V}$, $I_C = 100\text{ mA}$	-	7.0	-	V	
Collector-emitter saturation voltage	$V_{CE(sat)}$ (Terminal)	$V_{GE} = 15\text{ V}$, $I_C = 100\text{ A}$	$T_j = 25^\circ\text{C}$	-	1.95	-	V
			$T_j = 125^\circ\text{C}$	-	2.2	-	
	$V_{CE(sat)}$ (Chip)	$I_C = 100\text{ A}$	$T_j = 25^\circ\text{C}$	-	1.75	-	
			$T_j = 125^\circ\text{C}$	-	2.0	-	
Input capacitance	C_{ies}		-	13.3	-	nF	
Output capacitance	C_{oes}	$V_{GE} = 0\text{ V}$, $V_{CE} = 10\text{ V}$	-	0.8	-		
Reverse transfer capacitance	C_{res}	$f = 1\text{ MHz}$	-	1.2	-		
Turn-on time	t_{on}	$V_{CC} = 600\text{ V}$, $I_C = 100\text{ A}$	-	-	1.2	μs	
	t_r		-	-	0.6		
Turn-off time	t_{off}	$V_{GE} = \pm 15\text{ V}$, $R_g = 4.7\ \Omega$	-	-	1.0		
	t_f		-	-	0.3		
Diode forward voltage	V_F (Terminal)	$I_F = 100\text{ A}$	$T_j = 25^\circ\text{C}$	-	2.0	-	V
			$T_j = 125^\circ\text{C}$	-	2.0	-	
	V_F (Chip)	$I_F = 100\text{ A}$	$T_j = 25^\circ\text{C}$	-	1.8	-	
			$T_j = 125^\circ\text{C}$	-	1.8	-	
Reverse recovery time	t_{rr}	$I_F = 100\text{ A}$	-	-	0.35	μs	

(c) Thermal resistance characteristics

Item	Symbol	Condition	Characteristics			Unit
			min.	typ.	max.	
Thermal resistance (1 device)	$R_{th(j-e)}$	IGBT	-	-	0.21	$^\circ\text{C/W}$
		FWD	-	-	0.33	
Thermal resistance between case and fins	$R_{th(c-f)}$		-	0.05	-	

Table 2 1,200 V U-series IGBT modules

Rated voltage (V)	Package	Rated current (A)	Types	Sale date
1,200	Small PIM	10	7MBR10UE120	April 2003
		15	7MBR15UE120	
	EP2	10	7MBR10UA120	
		15	7MBR15UA120	
		25	7MBR25UA120	
		35	7MBR35UA120	
		35	7MBR35UB120	
	EP3	50	7MBR50UB120	
		75	7MBR75UB120	
		10	7MBR10UC120	
	HEP2	15	7MBR15UC120	
		25	7MBR25UC120	
		35	7MBR35UC120	
	HEP3	35	7MBR35UD120	
		50	7MBR50UD120	
		75	7MBR75UD120	
	New PC2	75	6MBI75UA-120	
		75	6MBI75UB-120	
	New PC3	100	6MBI100UB-120	
		150	6MBI150UB-120	
		75	6MBI75UC-120	
		100	6MBI100UC-120	
		150	3MBI150UC-120	
	New PC2	150	3MBI150U-120	
		7in1 (M631 or P611)	75	
	100		7MBI100UD-120	
	150		7MBI150UD-120	
	M232	75	2MBI75UA-120	
		100	2MBI100UA-120	
		150	2MBI150UA-120	
M233	150	2MBI150UB-120		
	200	2MBI200UB-120		
M234	200	2MBI200UC-120		
	300	2MBI300UC-120		
M235	300	2MBI300UD-120		
M238	300	2MBI300UE-120		
	450	2MBI450UE-120		
Large capacity module	225	6MBI225U-120		
	300	6MBI300U-120		
	450	6MBI450U-120		

Fig.8 Catalogue of packages of 1,200 V U-series

	PIM	6 in 1	7 in 1	2 in 1
EP2		PC3 	HEP2 	M232
EP3		Large capacity module 	HEP3 	M233
Small PIM1		M631 		M235
Small PIM2				M238

Fig.9 Correlation among 1,200 V U-series

Rated current	5A	10A	15A	25A (5.5kW)	35A (11kW)	50A (11kW)	75A (22kW)	100A (22kW)	150A (40kW)	200A (40kW)	300A (75kW)	450A (75kW)	600A
Series													
Small PIM	Small PIM												
PIM	EP2/HEP2		EP3/HEP3										
6 in 1			New PC3 with a thermal sensor (6 in 1)		M631 with a thermal sensor (7 in 1)		Large capacity module (6 in 1)						
2 in 1							M232		M233		M235		M238
/1 in 1													M138
PIM/6 in 1	For vector control	EP (N-line open)		New PC (with shunt resistance)									

3. Features of the New FWDs

As IGBT switching speeds have increased, the accompanying vibration at the time of switching has become a significant problem. Fuji Electric succeeded in realizing soft recovery to suppress the vibration even at a high di/dt by optimizing the surface structure and bulk impurities profile of the FWDs (free wheeling diodes) (Fig. 6).

Moreover, a newly developed FDW has been made suitable for parallel operation by optimizing a lifetime killer to achieve a positive temperature coefficient of the output characteristics (Fig. 7).

4. 1,200 V U-series IGBT Modules and Characteristics

Characteristics of 1,200 V U-series IGBT modules and an overview of U-series are presented in Tables 1

and 2, respectively. A catalog of packages available in this series is shown in Fig. 8 and the correlation among the 1,200 V U-series IGBT modules is shown in Fig. 9.

5. Conclusion

An overview of the 1,200 V U-series IGBT modules has been presented. The IGBTs of this series are extremely low loss devices and we believe they will make important contributions to the realization of

smaller size and lower loss equipment.

Fuji Electric intends to continue to work toward realizing higher performance and higher reliability devices and to contribute to the development of power electronics.

Reference

- (1) Laska, T. et al. The Field Stop IGBT (FS IGBT) — A New Power Device Concept with a Great Improvement Potential. Proc. 12th ISPSD. 2000, p 355-358.



U-series IGBT Modules (1,700 V)

Yasuyuki Hoshi
Yasushi Miyasaka
Kentaro Muramatsu

1. Introduction

In recent years, requirements have increased for high voltage power semiconductor devices used in high voltage power converters such as industrial inverters. The IGBT (insulated gate bipolar transistor), which has a high switching speed, low power dissipation loss and high voltage capability, has been replacing the conventionally used GTO (gate turn-off thyristor) and SCR. Advances in a comprehensive technological approach to IGBT design, including device design, process design and application design, have driven new IGBT development. The favorable response to market demands for economy and reliability serves to further promote the reputation of the IGBT.

Fuji Electric has recently developed a 1,700 V U-series IGBT in order to meet demands for larger current, smaller size and higher reliability. A trench structure is formed on the front surface and an FS (field stop) structure is formed on the back in order to achieve an improvement in the overall power loss. By optimizing characteristics of both structures, Fuji Electric succeeded in developing an IGBT that has very low power loss. In developing a highly responsive and low-loss IGBT, it was also necessary to improve characteristics of the FWD (free wheeling diode). The IGBT and FWD should be thought of as a single integrated unit. Fuji Electric has developed a FWD with soft recovery characteristics for noise reduction. This paper introduces the device characteristics and the product series of U-series IGBT modules.

2. Characteristics of the New IGBT

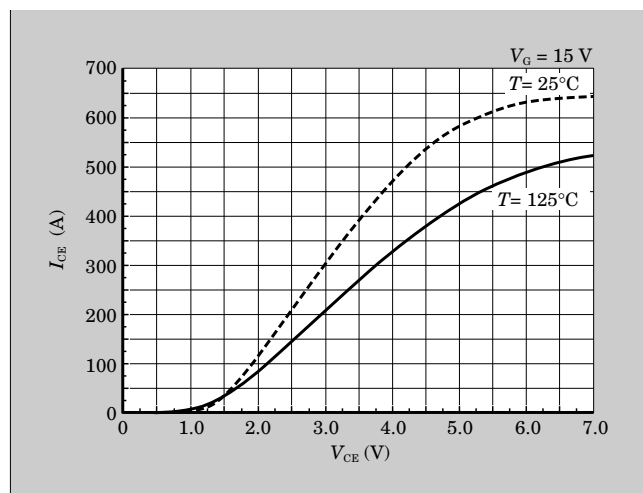
The surface of a conventional IGBT has a planer structure, therefore, its cell density is low and $V_{CE(sat)}$ is degraded by the J_{FET} resistance of this surface. Moreover, the NPT structure of the wafer substrate resulted in a thick wafer with a poor $V_{CE(sat)}-E_{off}$ tradeoff characteristic. The rated current density of the newly developed 1,700 V IGBT is set to over 130 A/cm², and the key development was increasing base current in the wide base transistor built into the IGBT. To optimize the surface structure, we run

simulations for front surface and back surface structures. Based on the results, we applied a trench structure to the surface. The trench structure eliminates J_{FET} resistance on the surface of the planer structure. Accompanying the increase in cell density, the electronic current from the surface increases, and a sufficient base current can be secured. Increasing the percentage of electron current among the total current enables turn off switching loss to be decreased.

Next, to achieve further improvement in the characteristics, we developed an FS structure and applied this structure to the IGBT. By applying the FS structure, resistance of the substrate wafer decreased, enabling both $V_{CE(sat)}$ and E_{off} to be reduced at the same time. The $V_{CE(sat)}-I_{CE}$ output characteristic is shown on the graph in Fig. 1.

Here, the salient feature is that even though a trench structure has been utilized, the saturation current is limited to 3.6 times the rated current and the saturation voltage is reduced to 2.5 V. The surface has not only been formed as a trench structure, but also, the cell pitch of the surface, especially the trench depth and V_{th} , have been optimized. As a result of improving both process and device technology, a low resistance IGBT has been developed. Consequently, the $V_{CE(sat)}-E_{off}$ tradeoff characteristic achieved signif-

Fig.1 Output characteristics of U-series IGBT (1,700 V/150 A)



icant improvement compared to a conventional structure (Fig. 2).

Figure 3 shows a turn-off waveform for an inductive load at 125°C and 150 A of rated current. When $V_{CE(sat)}$ is 2.5 V, the switching loss is 34 mJ. Figure 4 shows the turn-on waveform when di/dt is 2,700 A/ μ s.

Because trench and FS structures are utilized, the turn-on waveform is highly responsive. When $V_{CE(sat)}$ is 2.5 V, E_{on} is 31 mJ (Fig. 5). Figure 6 shows a waveform of the blocking voltage. The blocking voltage

is over 1,900 V and is sufficiently large.

Figure 7 shows a waveform of the SCSOA (short circuit safe operating area). When a short circuit occurs, the peak current is limited to about 600 A (4 times the rated current) and the SCSOA is capable of withstanding that current for 10 μ s. Previously, IGBTs with trench structures suffered from weak SCSOA withstand capability. However, the new 1,700 V U-

Fig.2 V_{on} vs. E_{off} characteristic of U-series IGBT

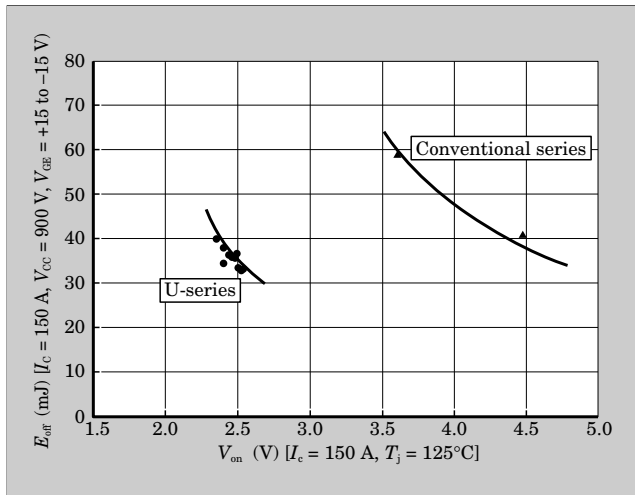


Fig.3 Turn-off waveform

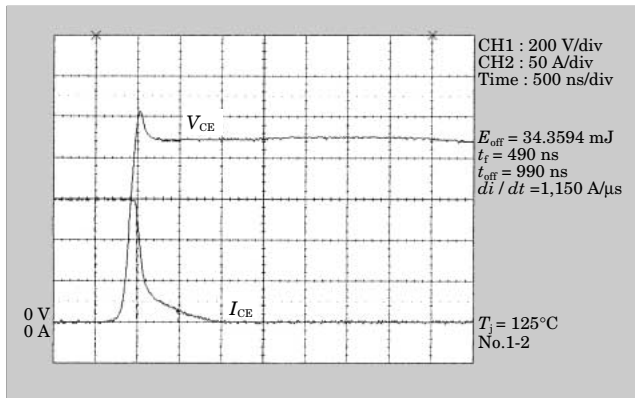


Fig.4 Turn-on waveform

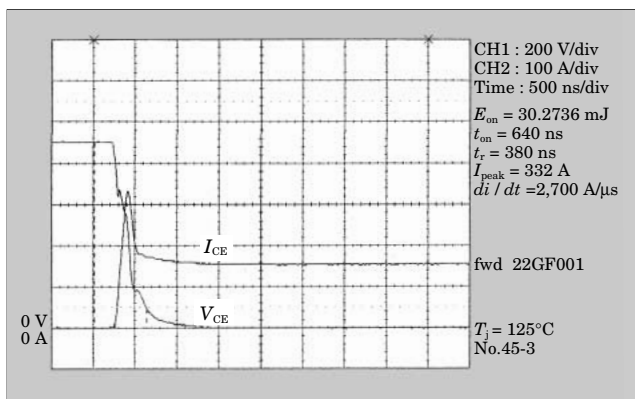


Fig.5 V_{on} vs. E_{on} characteristic of U-series IGBT

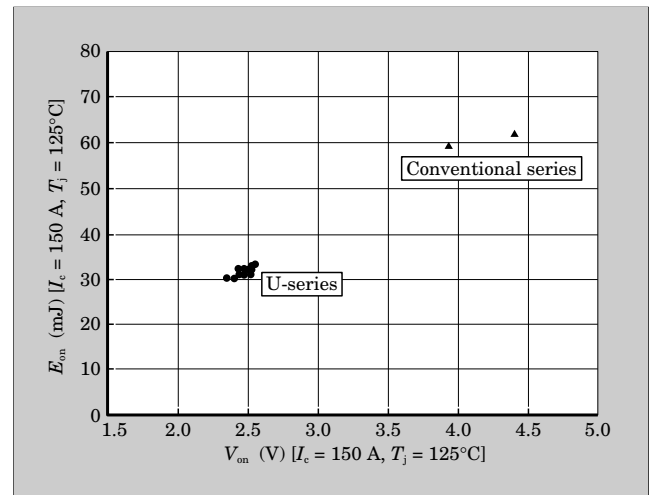


Fig.6 Waveform of blocking voltage

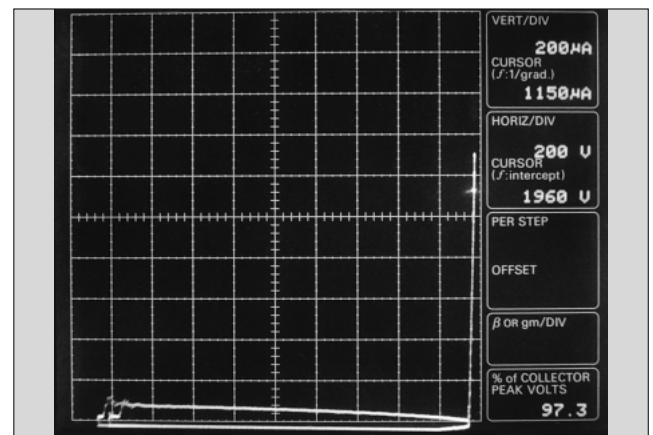


Fig.7 SCSOA waveform

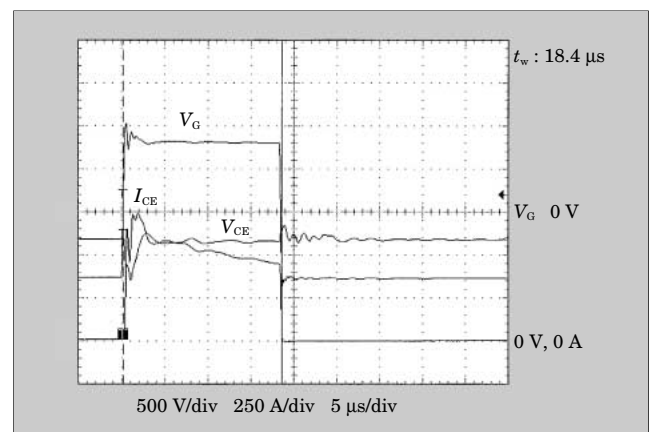


Fig.8 RBSOA locus

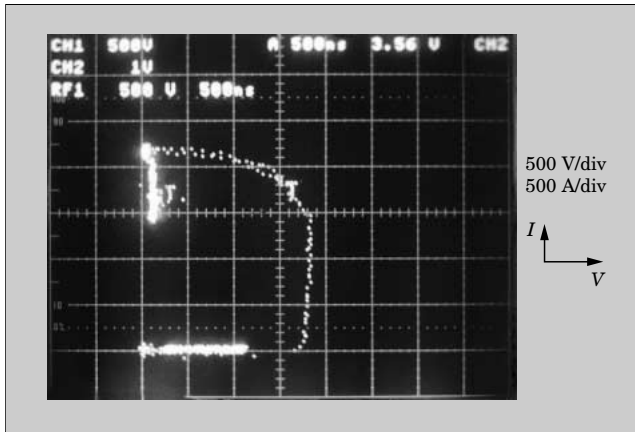
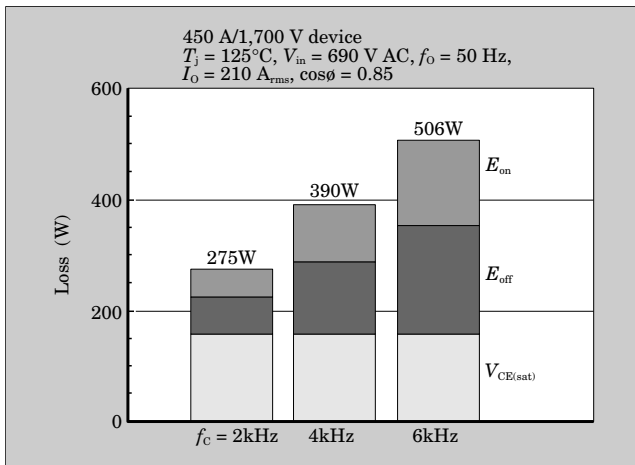


Fig.9 Power dissipation losses



series IGBT with its optimized surface trench structure possesses sufficient short circuit withstand capability. Figure 8 shows the RBSOA (reverse bias safe operating area) at 125°C. High withstand capability was verified at 8 times the rated current at $V_{CE} = 1,700$ V. Figure 9 shows the computed power loss for several carrier frequencies.

3. Characteristics of the New FWD

The IGBT module has a FWD connected back-to-back with an IGBT. Improvement of the FWD characteristics was also a very important factor. Improvement of the reverse recovery characteristics of the FWD when the IGBT is turned on was necessary in order to suppress the surge voltage rise, protect the IGBT and peripheral circuitry from damage and incorrect operation, and also to decrease turn-on loss. Moreover, in consideration of the reduced loss at the time of regeneration, decreasing V_F of the FWD has contributed to reducing the total loss of the product, and is very important. Economical efficiency is one of the most important considerations. The conventional FWD substrate design utilized an epitaxial wafer.

This time, in consideration of both economical

Fig.10 V_F - E_{tr} characteristics of U-series FWD

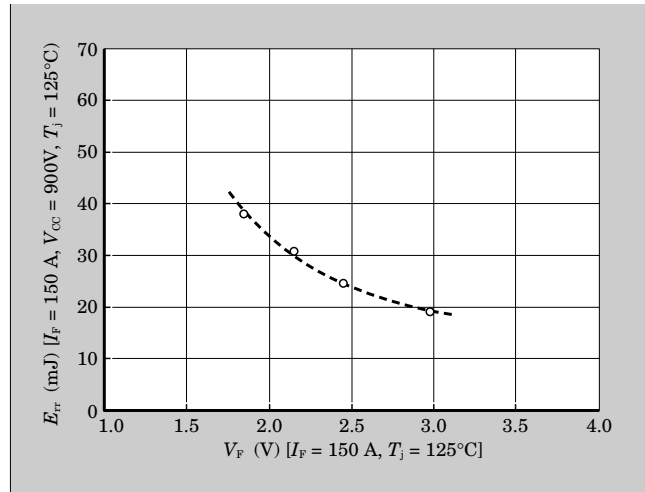


Fig.11 FWD output characteristics of U-series

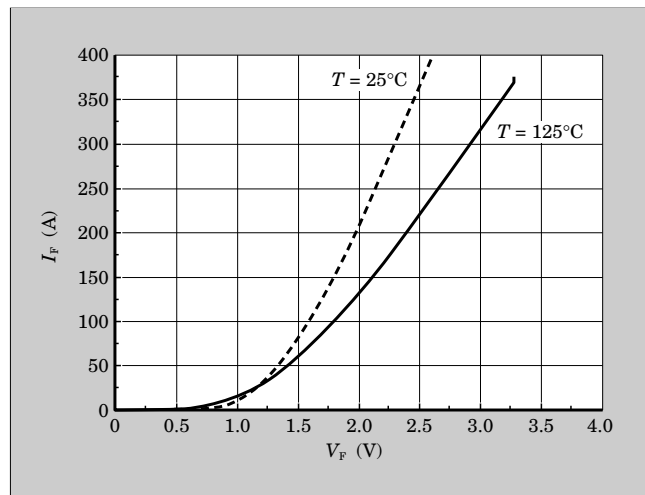
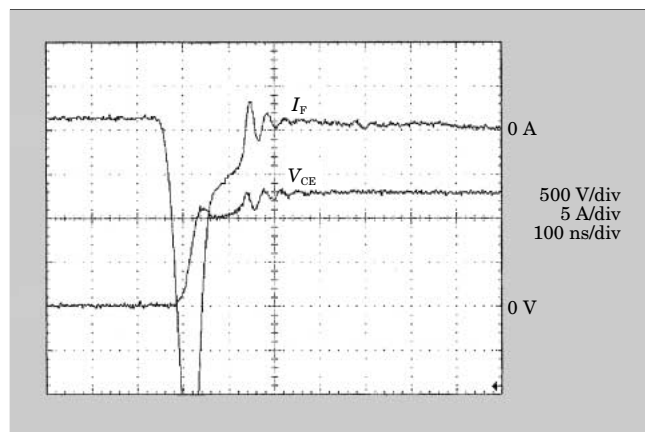


Fig.12 FWD reverse recovery waveform at low current



efficiency and total loss, a DW wafer was adopted and optimized to achieve characteristics comparable to the epitaxial wafer (Fig. 10).

Figure 11 shows the V_F - I_F characteristics. When incorporated into a large current rated product, as it was often used, the chip was connected in parallel, and

Fig.13 External appearance of ECONOPACK™-Plus

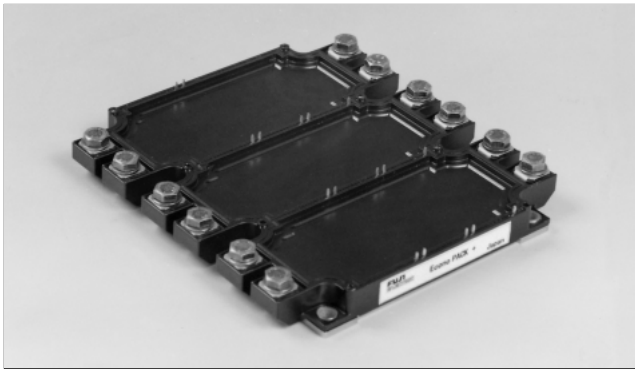


Fig.14 Outline drawing and equivalent circuit of ECONOPACK™-Plus

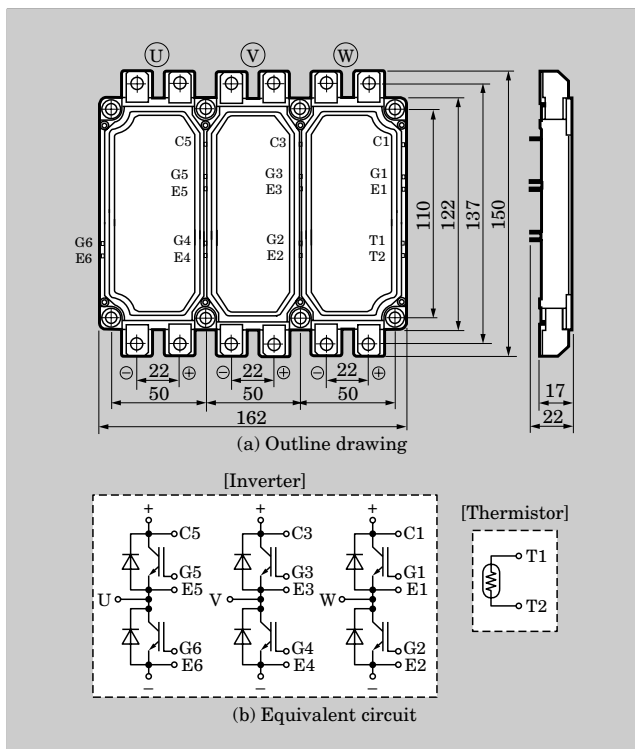


Table 1 1,700V U-series product lineup

Type	Item	Rated voltage	Rated current	Package number
	6MBI150U-170	1,700 V	150 A	M629
	6MBI225U-170		225 A	
	6MBI300U-170		300 A	
	6MBI450U-170		450 A	

when the temperature characteristic of forward voltage was negative, a current unbalance was easily generated, affecting the life cycle of the product. The newly developed U-series FWD utilizes a lifetime killer which makes the temperature characteristic of forward voltage positive. Figure 12 shows the reverse recovery

ECONOPACK™ is a trademark of eupec GmbH, Warstein.

Table 2 Ratings and characteristics of the 1,700 V / 450 A U-series

(a) Maximum rating (at $T_c=25^\circ\text{C}$ unless otherwise specified)
450 A/1,700 V device

Item	Symbol	Condition	Max. rating	Unit	
Collector-emitter voltage	V_{CES}		1,700	V	
Gate-emitter voltage	V_{GES}		± 20	V	
Collector current	I_C	Continuous	$T_j = 25^\circ\text{C}$	675	A
			$T_j = 80^\circ\text{C}$	450	
	$I_{C \text{ pulse}}$	1 ms	$T_j = 25^\circ\text{C}$	1,350	
			$T_j = 80^\circ\text{C}$	900	
	$-I_C$		450	A	
	$-I_{C \text{ pulse}}$		900	A	
Maximum loss	P_C	1 device	2,000	W	
Junction temperature	T_j		150	$^\circ\text{C}$	
Preserving temperature	T_{stg}		-40 to +125	$^\circ\text{C}$	
Isolation voltage (package)	V_{iso}	AC : 1 min	3,400	V AC	

(b) Electric characteristics (at $T_c=25^\circ\text{C}$ unless otherwise specified)
450 A/1,700 V device

Item	Symbol	Condition	Characteristics			Unit	
			min.	typ.	max.		
Zero gate voltage collector current	I_{CES}	$V_{GE} = 0 \text{ V}$, $V_{CE} = 1,700 \text{ V}$	-	-	3.0	mA	
Gate-emitter leakage current	I_{GES}	$V_{CE} = 0 \text{ V}$, $V_{GE} = \pm 20 \text{ V}$	-	-	0.6	μA	
Gate-emitter threshold voltage	$V_{GE(th)}$	$V_{CE} = 20 \text{ V}$, $I_C = 450 \text{ mA}$	TBD	7.0	TBD	V	
Collector-emitter saturation voltage	$V_{CE(sat)}$ -Chip	$V_{GE} = 15 \text{ V}$, $I_C = 450 \text{ A}$	$T_j = 25^\circ\text{C}$	-	2.20	TBD	V
			$T_j = 125^\circ\text{C}$	-	2.50	TBD	
Turn-on time	t_{on}	$V_{CC} = 900 \text{ V}$, $I_C = 450 \text{ A}$, $V_{GE} = \pm 15 \text{ V}$	t_{on}	-	-	1.2	μs
			t_r	-	-	0.6	
			$t_{r(i)}$	-	-	-	
Turn-off time	t_{off}	$R_g = \text{TBD } \Omega$	t_{off}	-	-	1.0	μs
			t_f	-	-	0.3	
Diode forward voltage	$V_{F\text{-Chip}}$	$V_{GE} = 0 \text{ V}$, $I_C = 450 \text{ A}$	$T_j = 25^\circ\text{C}$	-	1.75	-	V
			$T_j = 125^\circ\text{C}$	-	2.00	-	
Reverse recovery time	t_{rr}	$I_F = 450 \text{ A}$	-	-	0.35	μs	

(c) Thermal resistance characteristics 450A/1,700V device

Item	Symbol	Condition	Characteristics			Unit
			min.	typ.	max.	
Thermal resistance (1 device)	$R_{th(j-c)}$	IGBT	-	-	0.06	$^\circ\text{C/W}$
		FWD	-	-	0.10	
Thermal resistance between case and fins	$R_{th(c-f)}$		-	0.0167	-	$^\circ\text{C/W}$

waveform for 1/150th of the rated current. The U-series FWD has a surface construction that limits carrier injection, and by optimizing the DW wafer and selecting a high carrier injection from the cathode, the surge voltage can be limited to less than 1,700 V and favorable characteristics can be acquired.

4. Product Introduction

The newly developed 1,700 V U-series IGBT module, applied to ECONOPACK™-Plus and PIM (power integrated module) products, has a 50 % smaller footprint than conventional packages. The external appearance of the ECONOPACK™-Plus is shown in Fig. 13. Figure 14 shows an outline drawing of the ECONOPACK™-Plus and its equivalent circuit.

Table 1 lists the product lineup. The ratings and characteristics of the 1,700 V / 450 A module are shown in Table 2.

5. Conclusion

This paper has presented an overview of IGBT and FWD chip development and module products for the 1,700 V U-series. We believe that this IGBT and FWD can make a substantial contribution to meeting demands for smaller size, higher performance and higher reliability of devices. Although it was thought that characteristic improvement by means of trench technology would be difficult to implement for a high withstand voltage IGBT, a significant improvement in characteristics was achievable through optimization of the device technology. Fuji Electric will continue working to improve this technology further and to develop new products.

References

- (1) Sze, S. M. MODERN SEMICONDUCTOR DEVICE PHYSICS. 1st ed. USA. John Wiley & Sons. 1998, 557p.



R-IPM3 and Econo IPM Series of Intelligent Power Modules

Manabu Watanabe
Yoshiyuki Kusunoki
Naotaka Matsuda

1. Introduction

Fuji Electric has developed and mass-produced several series of IGBT-IPMs (insulated gate bipolar transistor-intelligent power modules), beginning with the J-series in 1993, followed by the N-series in 1995 and then the R-series in 1997. The J-series realized low loss, the N-series achieves soft switching and the R-series realized high reliability, high cost performance and improved protection accuracy by adopting a protection function to guard against overheating of the chip.

Against the backdrop of recent demands for higher frequency, smaller size, higher efficiency and lower noise requested of power electronics products, Fuji Electric has developed two new intelligent power modules, the R-IPM3, which is based on the R-IPM and provides improved loss characteristics, and the small and thin Econo IPM, which combines concepts of the R-IPM and Econo modules. This paper will introduce both of these modules.

For the IGBT, we developed a NPT (non punch through) microchip (T-series) having a thickness of 100 μm , which was realized by the establishment of a thin wafer process. For the FWD (free wheeling diode), we newly developed a new structure-FWD dies. This new FWD dies has an improved soft-recovery function. Table 1 lists the special features of each IPM series. We developed three series: the RTB type that has

improved cost performance, the Econo IPM that is realized in a small-size and thin package, and the RTA type that has a low loss level. In Fig. 1, external views of the R-IPM3, Econo IPM and small capacity R-IPM3 are shown.

2. R-IPM3 and Econo IPM Series

Table 2 lists the product series, characteristics and internal functions of the R-IPM3 and Econo IPM. IGBT dies adopted a NTP planer structure and attempted to reduce the switching loss. FWD dies optimized the anode structure and further improved the soft-recovery function.

The R-IPM3 series has external dimensions and functions that are interchangeable with the prior R-IPM series, and consequently, it is the most suitable replacement.

The Econo IPM series minimized its external dimensions and decreased its footprint by about 30 % compared to the conventional R-IPM. Further, by adding the upper arm alarm output, more reliable protection against a grounding fault can be realized.

For both of these series, we prepared a 6-in-1 module set and a 7-in-1 module set (including a built-in IGBT for braking) with 50 to 150 A of rated current for the 600 V class modules. Further, for 20 A low

Table 1 Special features of IPM

Item	Series name		Econo IPM	Low capacity R-IPM3
	RTA	RTB		
External dimensions	<ul style="list-style-type: none"> Interchangeable with R-IPM series (Standard package) Screw terminal 		<ul style="list-style-type: none"> Small size, thin-type Pin terminal 	<ul style="list-style-type: none"> Package with copper base Small size
Special feature	<ul style="list-style-type: none"> Low power dissipation (18 % less than R-IPM) 	<ul style="list-style-type: none"> Low power dissipation (10 % less than R-IPM) Cost performance 	<ul style="list-style-type: none"> Low power dissipation (10 % less than R-IPM) Cost performance 	<ul style="list-style-type: none"> Heat dissipation was improved with base. (Compared to baseless module)

Fig.1 External view of IPM

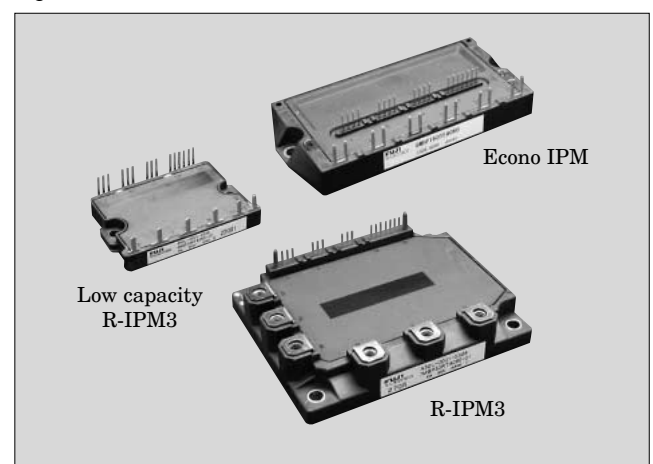


Table 2 Series, special characteristics and internal functions of IPM

(a) Econo IPM

Number of elements	Model	V_{DC} (V)	V_{CES} (V)	Inverter part		Brake part		Internal function							Package type		
				I_C (A)	P_C (W)	I_C (A)	P_C (W)	Upper and lower arms common			Upper arm		Lower arm			TcOH	
								Dr	UV	TjOH	OC	ALM	OC	ALM			
6 in 1	6MBP 50TEA060	450	600	50	144	-	-	○	○	○	○	○	○	○	○	×	P622
	6MBP 75TEA060			75	198	-	-	○	○	○	○	○	○	○	○	×	
	6MBP 100TEA060			100	347	-	-	○	○	○	○	○	○	○	○	×	
	6MBP 150TEA060			150	431	-	-	○	○	○	○	○	○	○	○	×	
7 in 1	7MBP 50TEA060	450	600	50	144	30	144	○	○	○	○	○	○	○	○	×	P622
	7MBP 75TEA060			75	198	50	198	○	○	○	○	○	○	○	○	×	
	7MBP 100TEA060			100	347	50	198	○	○	○	○	○	○	○	○	×	
	7MBP 150TEA060			150	431	50	198	○	○	○	○	○	○	○	○	×	

(b) R-IPM3

Number of elements	Model	V_{DC} (V)	V_{CES} (V)	Inverter part		Brake part		Internal function							Package type	
				I_C (A)	P_C (W)	I_C (A)	P_C (W)	Upper and lower arms common			Upper arm		Lower arm			TcOH
								Dr	UV	TjOH	OC	ALM	OC	ALM		
6 in 1	6MBP 20RTA060*	450	600	20	103	-	-	○	○	○	×	×	○	○	×	P619
	6MBP 50RTA060			50	198	-	-	○	○	○	○	×	○	○	○	P610
	6MBP 80RTA060			80	347	-	-	○	○	○	○	×	○	○	○	P611
	6MBP 100RTA060			100	431	-	-	○	○	○	○	×	○	○	○	
	6MBP 160RTA060			160	500	-	-	○	○	○	○	×	○	○	○	
	6MBP 50RTB060			50	144	-	-	○	○	○	○	×	○	○	○	P610
	6MBP 75RTB060			75	198	-	-	○	○	○	○	×	○	○	○	P611
	6MBP 100RTB060			100	347	-	-	○	○	○	○	×	○	○	○	
	6MBP 150RTB060			150	431	-	-	○	○	○	○	×	○	○	○	
7 in 1	7MBP 50RTA060	450	600	50	198	30	144	○	○	○	○	×	○	○	○	P610
	7MBP 80RTA060			80	347	50	198	○	○	○	○	×	○	○	○	
	7MBP 100RTA060			100	431	50	198	○	○	○	○	×	○	○	○	P611
	7MBP 160RTA060			160	500	50	198	○	○	○	○	×	○	○	○	P610
	7MBP 50RTB060			50	144	30	144	○	○	○	○	×	○	○	○	
	7MBP 75RTB060			75	198	50	198	○	○	○	○	×	○	○	○	
	7MBP 100RTB060			100	347	50	198	○	○	○	○	×	○	○	○	P611
	7MBP 150RTB060			150	431	50	198	○	○	○	○	×	○	○	○	

Dr : IGBT Driving circuit, UV : Under voltage lockout for control circuit, TjOH : Protection for device heating, OC : Overcurrent protection, ALM : Alarm output,

TcOH : Protection for case temperature

* 6MBP20RTA060 : Adopt detection method by shunt resistance at N line.

capacity elements, we improved the ease of use by using a copper base type package. Consequently, the user can select an appropriate product from a diverse product line-up. Figure 2 shows the external view of each IPM.

3. Special Features of the Power Devices

Cross-sectional views of the PT (punch through)-IGBT applied to the prior R-IPM and the NPT-IGBT applied to the R-IPM3 and Econo IPM are shown in Fig. 3.

The three special features of the NPT-IGBT are as follows:

(1) The saturation voltage between collector and

emitter ($V_{CE(sat)}$) has a positive temperature coefficient, and consequently current does not concentrate in a unit cell in the chip.

(2) The temperature dependency of turn-off loss (E_{off}) is small.

(3) There is no lifetime control, and consequently the fluctuation of ($V_{CE(sat)}$) is small.

The trade-off relation between $V_{CE(sat)}$ and turn-off loss is shown in Fig. 4. From Fig. 4, it can be seen that the prior IGBT chip's N-series and S-series have a high temperature dependence. On the other hand, the newly developed NPT planer chip mounted T-series has low temperature dependence, and therefore can reduce the turn-off loss at high temperatures.

Figure 5 compares the fluctuation of $V_{CE(sat)}$,

Fig.2 External dimensions of IPM

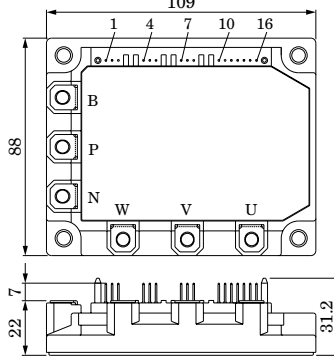
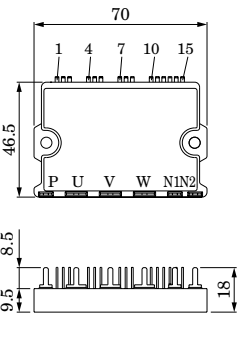
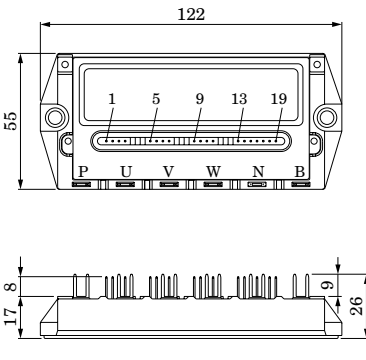
Series name	R-IPM3		Econo IPM
Package type	P610, P611	P619	P622
Outline drawings			
	Dimensions	L109×W88×H22 (mm)	L70×W46.5×H9.5 (mm)
Mass	450g	85g	270g

Fig.3 Comparison of IGBT chip cross-sections

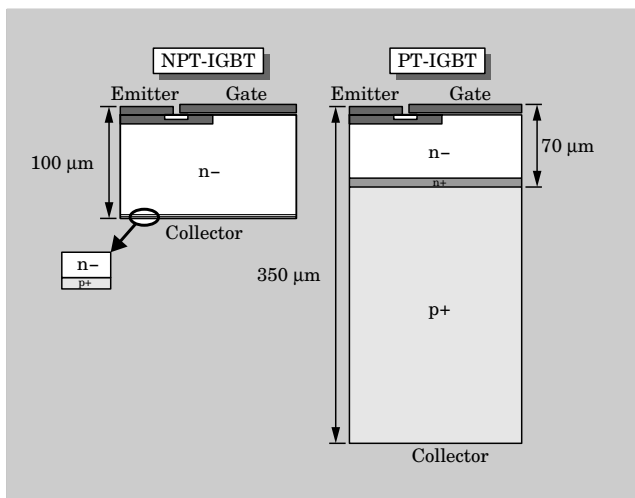


Fig.4 Trade-off curve of IGBT chips

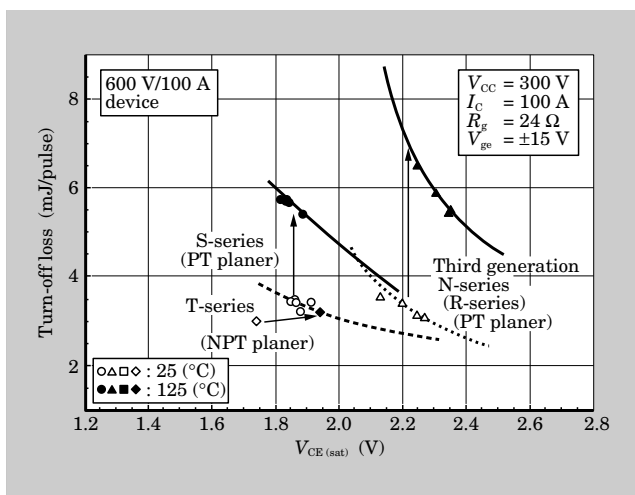


Fig.5 Distribution chart of $V_{CE(sat)}$

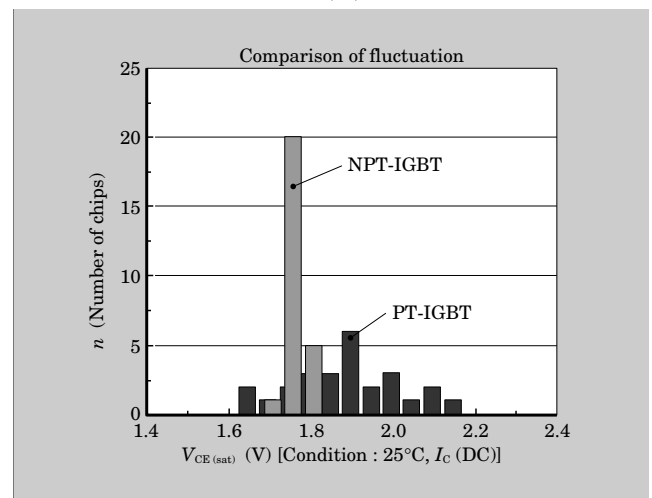
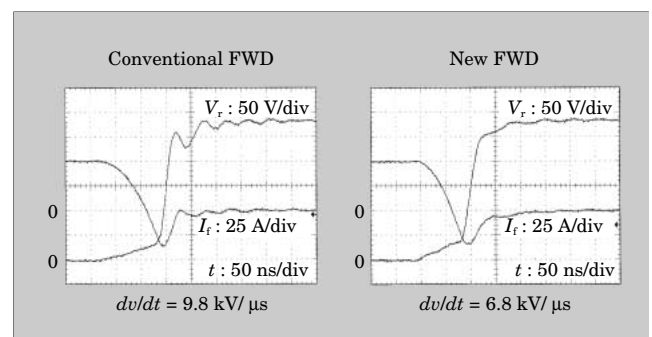


Fig.6 Comparison of recovery switching waveform of FWD between conventional FWD and new FWD



between the PT-planer chip and the NPT-planer chip. $V_{CE(sat)}$ of the NPT-planer chip is distributed in a limited range and exhibits stable, steady-state loss

characteristics.

Next, we shall describe the FWD that has been utilized in the R-IPM3 and Econo IPM. Fuji Electric applied the new structure to the FWD in order to decrease emission noise. Figure 6 shows comparison of recovery switching waveform of FWD between conventional FWD and new FWD. New structure FWD achieves, that suppress the injection of holes from the anode and decrease the reverse recovery peak current to achieve soft recovery.

Fig.7 Internal construction of Econo IPM

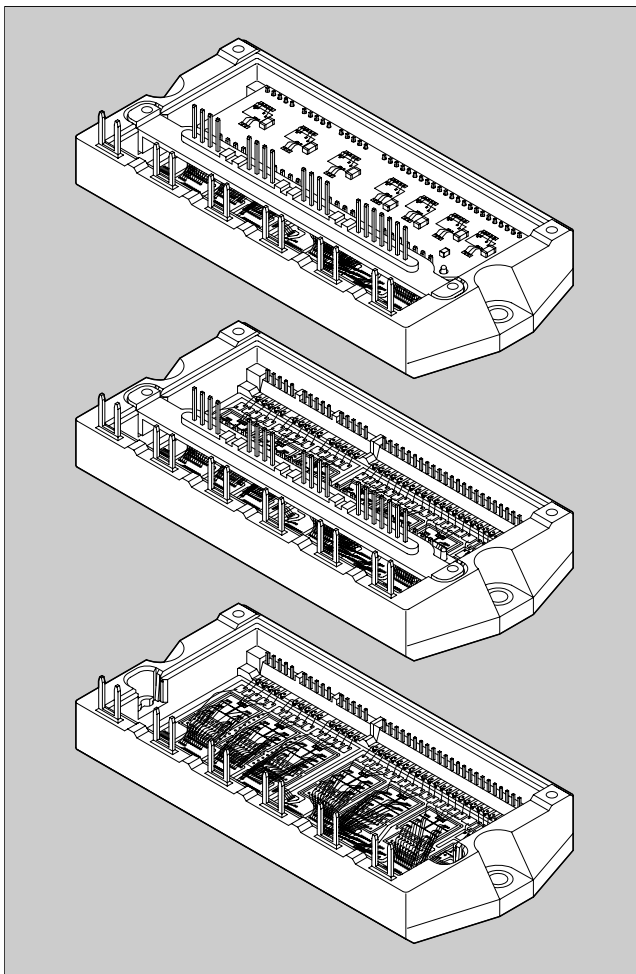
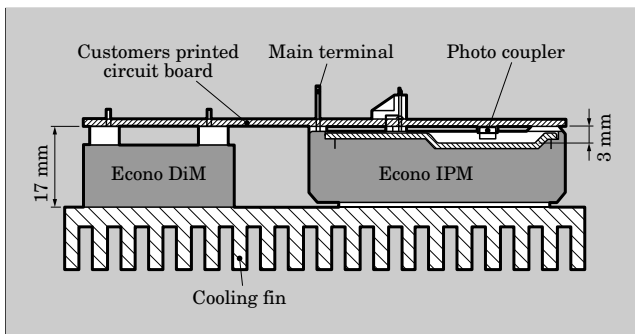


Fig.8 Example of Econo IPM installation



4. Package Construction

In order to achieve smaller and thinner dimensions, the Econo IPM is manufactured with a different construction than the prior IPM. In the prior package, a terminal bar was used for the interconnects. But with that method, the height of package cannot be decreased because of the limitations of the bar interconnects. For this reason, the Econo IPM changed from a terminal bar construction to a method of using

Fig.9 Comparison of total loss

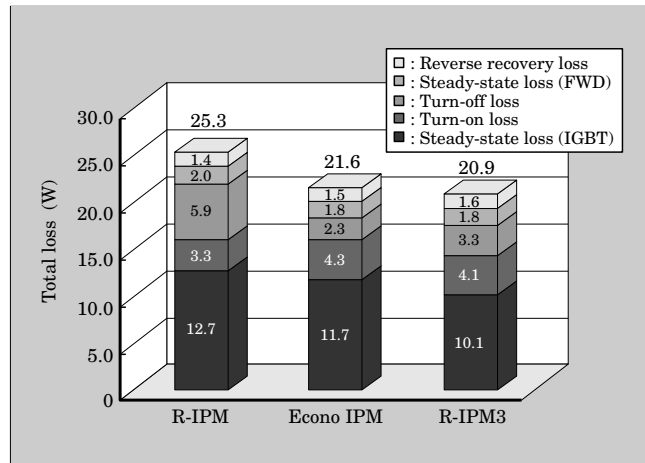


Fig.10 Turn-off waveform

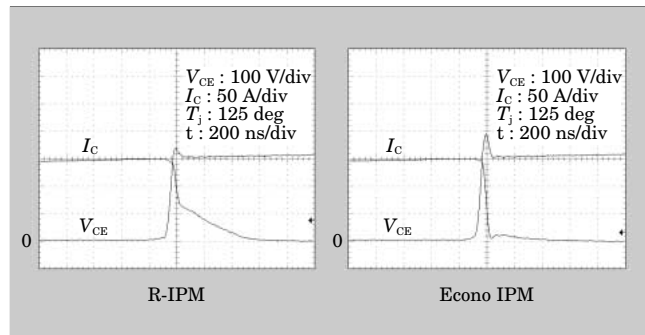


Fig.11 Comparison of the spectrum of emission noise

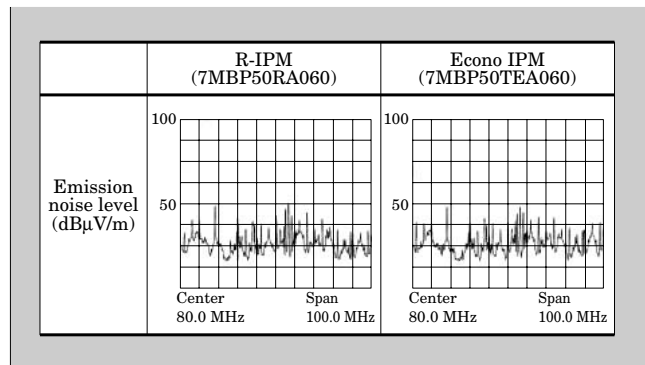
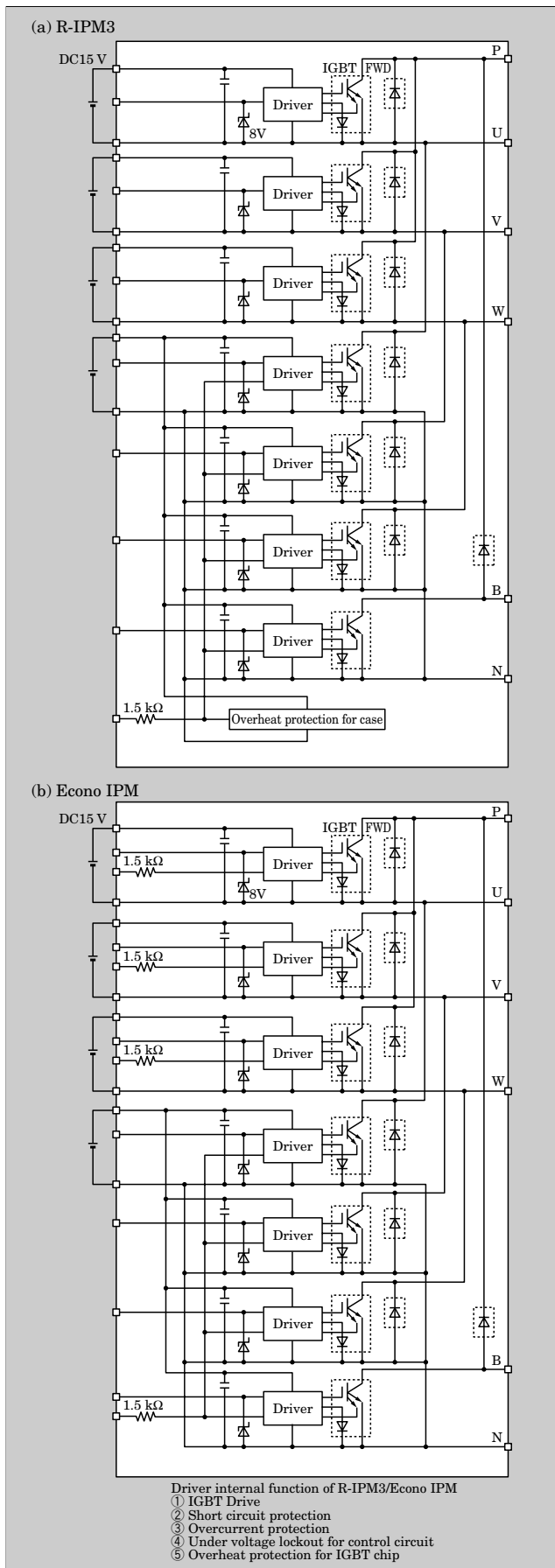


Fig.12 Block diagram of IPM circuit



aluminum wires for all internal interconnects. Further, to limit the package width, we introduced a construction wherein the control card printed circuit board is positioned on the second level. By adopting these changes, we succeeded in manufacturing a very compact package (see Fig. 7).

Figure 8 shows an example of an Econo IPM installed in a side-fin type servo-amp. The Econo-DiM (Econo Diode Module) in this drawing was developed with the same concept (the Econo-module concept) as the Econo IPM, and therefore has the same height of 17 mm as the Econo IPM. Since the Econo IPM and Econo-DiM have the same height, they can be connected on the same printed circuit board. By utilizing these two modules, simplification of the design of printed circuit boards can be expected. Further, in order to utilize the thin package more effectively, the Econo IPM reduces the height of a part of its lid. By ensuring a 3 mm space between the printed circuit board and the Econo IPM lid, the mounting of electronics components such as a photo-coupler on the back of the printed circuit board is possible. Consequently, it is expected that dead space in customers' equipment can be decreased, further contributing to reducing the footprint customer's equipment.

5. Reduction of Loss

As product development concepts, the reduction of loss and the level of emission noise, which have a mutual tradeoff relationship, are the most important items.

These items were one of the important themes of the newly developed Econo IPM and R-IPM3 modules. During development, we were able to decrease IGBT loss by adopting the newly developed NPT-IGBT, and moreover, by installing a new diode that has a soft-recovery function and by optimizing the driving conditions, we succeeded in realizing the same or lower noise level than the prior R-IPM.

Figure 9 compares total loss between the newly developed Econo IPM, R-IPM3 and the prior R-IPM. As a result of installing the new IGBT chip and FWD chip, loss decreases of 15 % in the Econo IPM and 18 % in the R-IPM3, compared to the prior R-IPM, were realized. In particular, the decrease in turn-off loss greatly contributed to the decrease in total loss. Figure 10 shows turn-off waveforms of the prior IPM and Econo IPM. Figure 11 shows the emission noise spectrum of the R-IPM and Econo IPM. The emission noise spectrum was measured by the 3 m method for accelerating and decelerating operation utilizing a servo-amp with a 4 kHz carrier frequency. Consequently, it was learned that the noise level is kept at the same level as the prior type over the frequency range from 30 to 130 MHz.

6. Block Diagram of IPM

Figure 12 shows block diagrams of modules with built-in dynamic brake functions. Figure 12(a) is the R-IPM3, and 12(b) is the Econo IPM. In case of Econo IPM, the alarm signal of the upper arm circuit is output externally.

7. Conclusion

IGBT-IPMs which incorporate the latest power device technology from Fuji Electric have been presented. We are convinced that these IPMs will enable the

development of highly efficient and small size power electronics application products and will satisfy the market expectations.

We at Fuji Electric will continue to develop and produce new products in order to meet the requirements of markets in the future.

References

- (1) Kusunoki, Y. et al. A new compact intelligent power module with high reliability for servo drive application. PCIM Europe 2002.
- (2) Matsuda, N. et al. New 600V Compact Intelligent Power Module "Econo IPM". CIPS2002, p.101-106.



SuperFAP-G Series of Power MOSFETs

Hiroyuki Tokunishi
Tadanori Yamada
Masanori Inoue

1. Introduction

In recent years, shipments of information and communication equipment, mainly network related equipment such as personal computers and servers, have been rapidly increasing as IT (information technology) progresses. Accordingly, reduction of power dissipation in the equipment is strongly required in order to achieve resource-saving, energy-saving and downsizing. The SMPS (switched mode power supply) used in this equipment is required to have high efficiency and low loss. Moreover, for OA (office automation) equipment that has long standby times, such as facsimile and copy machines, a reduction of the power dissipation during standby is also required, and the trend toward higher efficiency and lower loss is growing, supported with regulations such as the revised energy-saving law.

Figure 1 shows the simulated results of power MOSFET (metal oxide semiconductor field effect transistor) loss in a forward converter, a typical SMPS. The turn-off loss constitutes about 50 % of the total loss under the steady load condition (output current of 8 A). Moreover, the on-state resistance ($R_{DS(on)}$) loss

constitutes about 32 % of the total loss. Thus, 80 % or more of the total loss is comprised of the turn-off loss and the on-state resistance loss. This fact demonstrates the necessity of improving both types of loss in order to achieve high efficiency and low loss of an SMPS. On the other hand, the turn-off loss constitutes about 90 % of the total loss at a light load condition equal to the standby power dissipation. To accommodate downsizing of the information and communication equipment, SMPS is adopting high switching frequency, and the trend in recent years has been toward even higher frequencies. In the future, reduction of the switching loss, typified by the turn-off loss, is expected to become even more important.

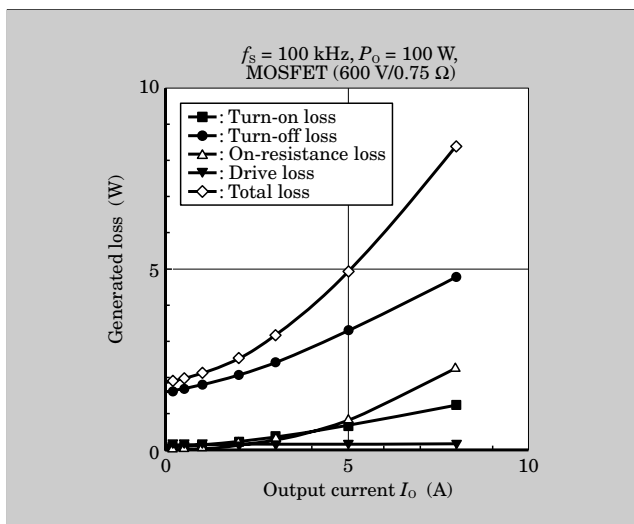
This paper will present an overview of the features of the low loss and ultra-high speed power MOSFET SuperFAP-G series, developed to satisfy the abovementioned market needs, and its effectiveness in applications.

2. Features

The turn-off loss of a power MOSFET is determined by the charging time constant of the reverse transfer capacitance (C_{rss}) between the drain and gate. Accordingly, the amount of electric charge (Q_{gd}) between the drain and gate must be reduced in order to decrease the turn-off loss. There is a trade-off relationship between Q_{gd} and $R_{DS(on)}$ and improvement of the trade-off is essential to achieve the desired power MOSFET specifications of reduced on-state resistance and turn-off loss. Accordingly, the definition of the figure-of-merit (FOM) of a power MOSFET, previously represented as $R_{on} \cdot A$, has been reestablished as the product of $R_{DS(on)}$ and Q_{gd} . This means that a smaller value of $R_{on} \cdot Q_{gd}$ indicates a higher performance power MOSFET.

In Table 1, characteristics of a SuperFAP-G device are compared with those of a conventional product having the same on-state resistance. The representative model, newly developed and having a drain-source breakdown voltage of 150 V, has a FOM of $0.675 \Omega \cdot nC$, indicating that performance has been improved by about 2.5 times compared to the conven-

Fig.1 Simulation results of forward converter loss



tional product. Design techniques for realizing such improvement in the FOM will be described below.

3. Design Technologies

In the SuperFAP-G series, a new technique referred to as quasi-planar-junction (QPJ) was developed to improve the on-state resistance loss. Figure 2 shows the structure of the QPJ.

Most of the on-state resistance in a power MOSFET with medium or high drain-source voltage is limited by the resistivity of n- type silicon in the epitaxial layers. Therefore, reducing n- type silicon resistivity achieves low on-state resistance, but this approach leads to the problem of decreased drain-source breakdown voltage. Theoretically, the on-state resistance per unit area ($R_{on} \cdot A$) is proportional to the 2.5th power of the breakdown voltage, so low resistivity n- type silicon, near the theoretical limit, must be used to decrease the on-state resistance of power MOSFETs as much as possible. The cell structure of a conventional power MOSFET contains much three-dimensional unevenness and therefore the electric

field is highly concentrated and only about 80 % of the theoretical limit of the breakdown voltage had been achieved. To supplement the voltage, it was necessary to increase n- type silicon resistivity to more than 175 % of the theoretical limit, but as a consequence, the on-state resistance per unit area could not be decreased. In the QPJ structure of the SuperFAP-G series, a cell with a junction having a nearly planar surface has been realized by arranging low-concentration shallow p- wells densely, in place of the conventional high-concentration deep p+ wells. The QPJ structure has achieved a breakdown voltage of 97 % relative to the silicon theoretical limit, and as a result, has reduced the n- type silicon resistivity to 108 % of the theoretical limit and achieved low on-state resistance within 10 % of the silicon theoretical limit value shown in Fig. 3. On the other hand, in order to reduce

Table 1 Comparison of SuperFAP-G characteristics

Item	Series	SuperFAP-G 2SK3474-01	Conventional product 2SK2226-01
V_{DS}		150 V	150 V
I_D		33 A	20 A
P_D		150 W	80 W
$V_{GS(th)}$		3 to 5 V	1 to 2.5 V
$R_{DS(on)(typ.)}$		54 mΩ	55 mΩ
Q_g		34 nC	100 nC
Q_{gd}		12.5 nC	30 nC
FOM $R_{on} \cdot Q_{gd}$		0.675 Ω · nC	1.65 Ω · nC

Fig.3 Relation between V_b and $R_{on} \cdot A$

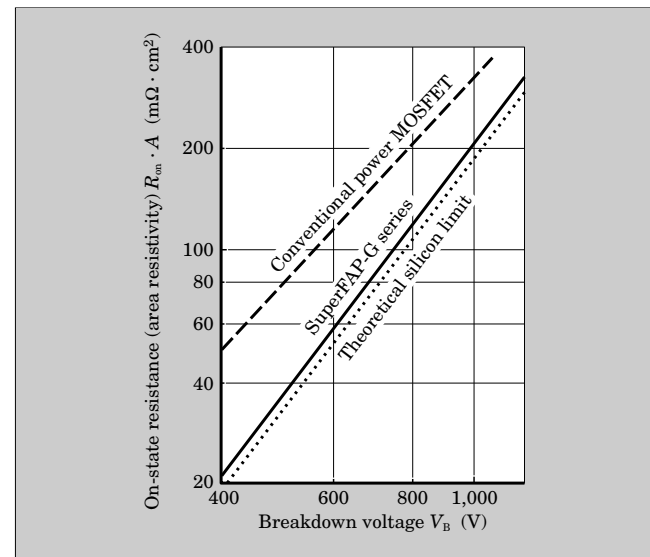


Fig.2 SuperFAP-G chip structure (QPJ structure)

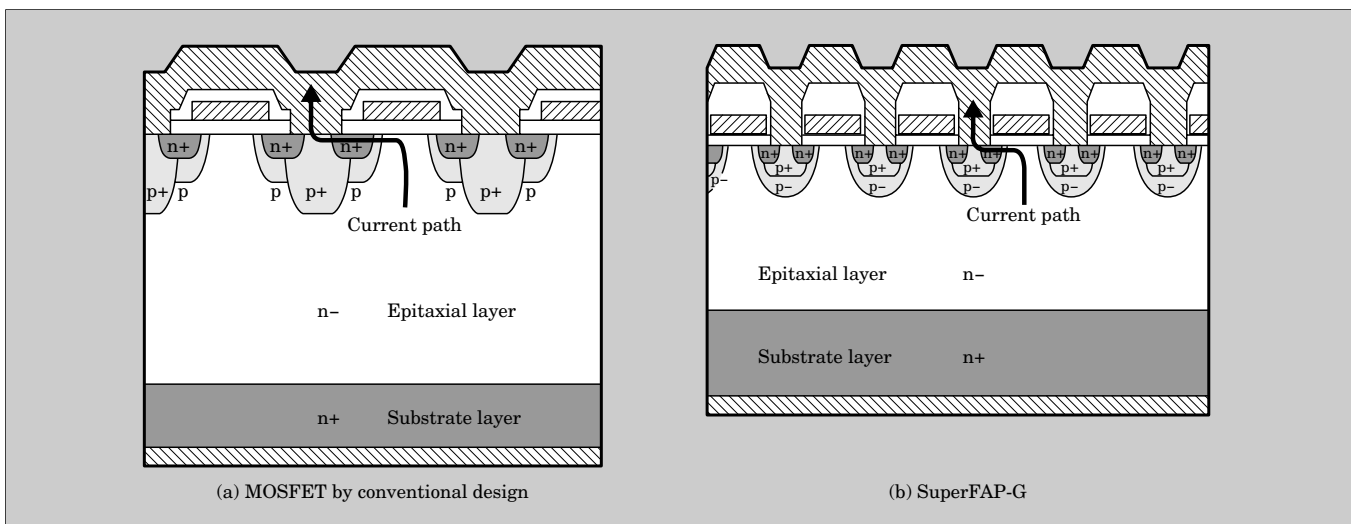


Table 2 SuperFAP-G series

Drain-source voltage BV_{DSS}	Drain current I_D	On-state resistance $R_{DS(on)}$ (max.)	Gate charge		Package				
			Q_G	Q_{gd}	TO-220	TO-220F	D ² -pack	TFP	TO-247
100 V	29 A	62 mΩ	22 nC	6 nC	2SK3598	2SK3599	2SK3600	2SK3601	–
	41 A	44 mΩ	32 nC	9 nC	2SK3644	2SK3645	2SK3646	2SK3647	–
	73 A	25 mΩ	52 nC	18 nC	2SK3586	2SK3587	2SK3588	2SK3589	–
150 V	23 A	105 mΩ	21 nC	6 nC	2SK3602	2SK3603	2SK3604	2SK3605	–
	33 A	70 mΩ	34 nC	12.5 nC	2SK3648	2SK3649	2SK3650	2SK3474	–
	57 A	41 mΩ	52 nC	18 nC	2SK3590	2SK3591	2SK3592	2SK3593	–
200 V	18 A	170 mΩ	21 nC	5 nC	2SK3606	2SK3607	2SK3608	2SK3609	–
	45 A	66 mΩ	51 nC	16 nC	2SK3594	2SK3595	2SK3596	2SK3597	–
250 V	14 A	260 mΩ	21 nC	5 nC	2SK3610	2SK3611	2SK3612	2SK3613	–
	37 A	100 mΩ	44 nC	16 nC	2SK3554	2SK3555	2SK3556	2SK3535	–
700 V	10 A	1.18 Ω	35 nC	10 nC	–	2SK3673	–	–	–
	12 A	0.93 Ω	31 nC	9 nC	–	2SK3577	–	–	–
800 V	7 A	1.9 Ω	25 nC	7 nC	2SK3529	2SK3530	–	–	–
900 V	6 A	2.5 Ω	25 nC	7 nC	2SK3531	2SK3532	2SK3676	–	–
	7 A	2.0 Ω	28 nC	8 nC	2SK3533	2SK3534	2SK3674	–	2SK3675
	9 A	1.58 Ω	32 nC	7 nC	2SK3678	2SK3679	–	–	–
	10 A	1.4 Ω	37 nC	10 nC	–	–	–	–	2SK3549

Fig.4 External view of SuperFAP-G

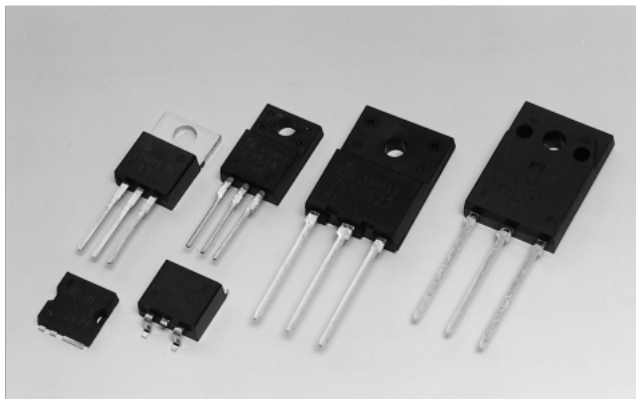
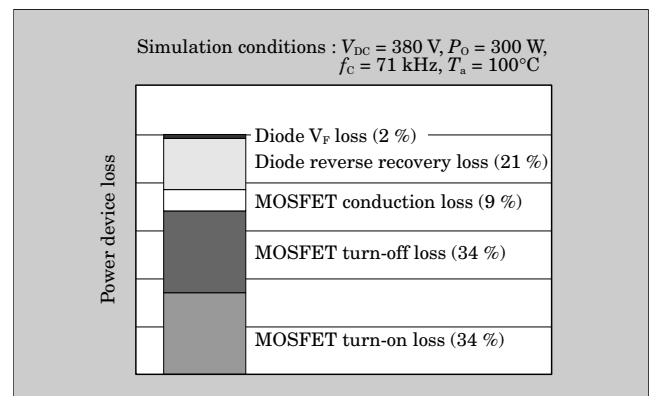


Fig.5 Simulation results of loss in continuous current mode PFC circuit



Q_{gd} that determines the turn-off loss, it is necessary to narrow the n- type silicon width (current path) and make it shorter. However, there is a trade-off relationship between Q_{gd} and $R_{DS(on)}$, and a narrower current path creates the problem of increased on-state resistance. In the QPJ structure, in addition to shortening the current path with shallow p- wells, high-concentration n type doping narrows the n- type silicon current path to its limit without increasing the on-state resistance. As a result, Q_{gd} has been reduced by about 60 % compared to conventional products with the same on-state resistance.

3.1 SuperFAP-G series

In the SuperFAP-G series, about 40 types of products with drain-source voltage range from 450 to 600 V have been developed and are already being

commercially produced. The following products have been added to the product series at this time: 100 to 250 V, medium drain-source voltage class power MOSFETs for use in DC-DC converters supporting a 12 to 72 V DC input, and 700 to 900 V drain-source voltage class power MOSFETs for use in SMPS with a 200 V AC input. Typical ratings of the SuperFAP-G series newly added to the product line are shown in Table 2. External views of the SuperFAP-G series are shown in Fig. 4.

4. Application and Merit of SuperFAP-G Series

As example applications, the results of applying the newly developed SuperFAP-G series in typical circuits, such as PFC (power factor correction) and DC-

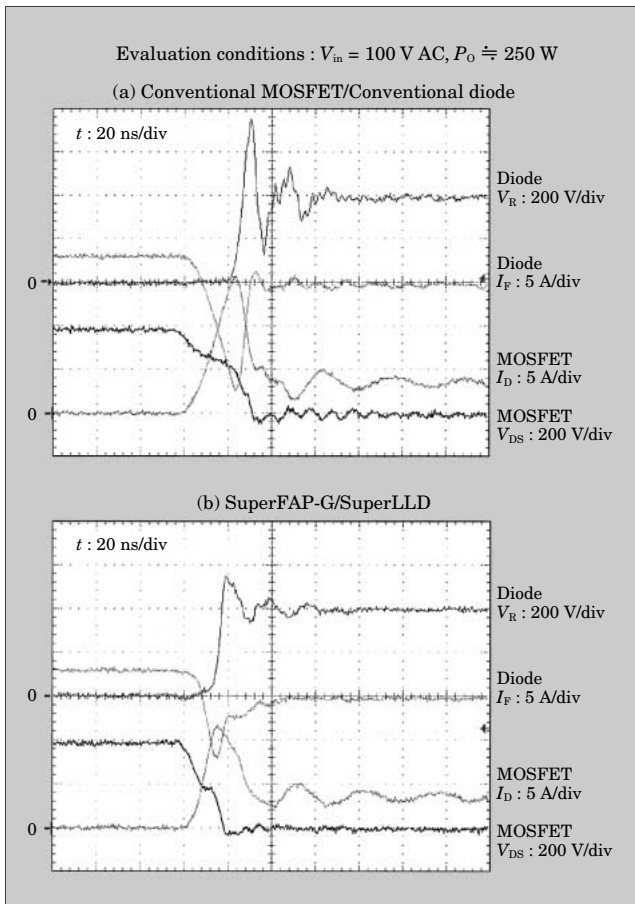
DC converter circuits, will be introduced below.

4.1 Application to PFC circuit

A capacitor-input type SMPS is usually equipped with a PFC circuit using a booster type converter to regulate input higher harmonic current. The addition of a PFC circuit means that the power-conversion circuit will be in two blocks, so loss reduction and efficiency improvement in the PFC circuit are strongly required. Figure 5 shows analyzed results of the loss generated from switching devices in a continuous current mode PFC circuit. The power MOSFET loss constitutes about 70 % of the generated loss, and 90 % of which is attributed to both of the turn-on and turn-off switching loss.

As shown in Fig. 6, the turn-on loss of a power MOSFET is strongly affected by reverse recovery characteristics of the output diode in a continuous current mode PFC circuit. Thus, in order to reduce the turn-on loss, it is important to decrease the reverse recovery current of the diode (I_{rr}). We have developed and commercialized the super high-speed diode SuperLLD series, having improved reverse recovery characteristics and designed for optimum use of continuous current mode PFCs. Use of the SuperLLD series reduces the turn-on loss of a power MOSFET by about

Fig.6 Continuous current mode PFC circuit (turn-on waveform)



40 % compared with conventional diodes.

On the other hand, turn-off loss, as shown by the waveforms in Fig. 7, is determined by the switching characteristics of the power MOSFET itself. Application of the SuperFAP-G series allows the turn-off time to speed up by about 60 % and the generated loss to decrease by about 80 % compared with conventional power MOSFETs having the same rating.

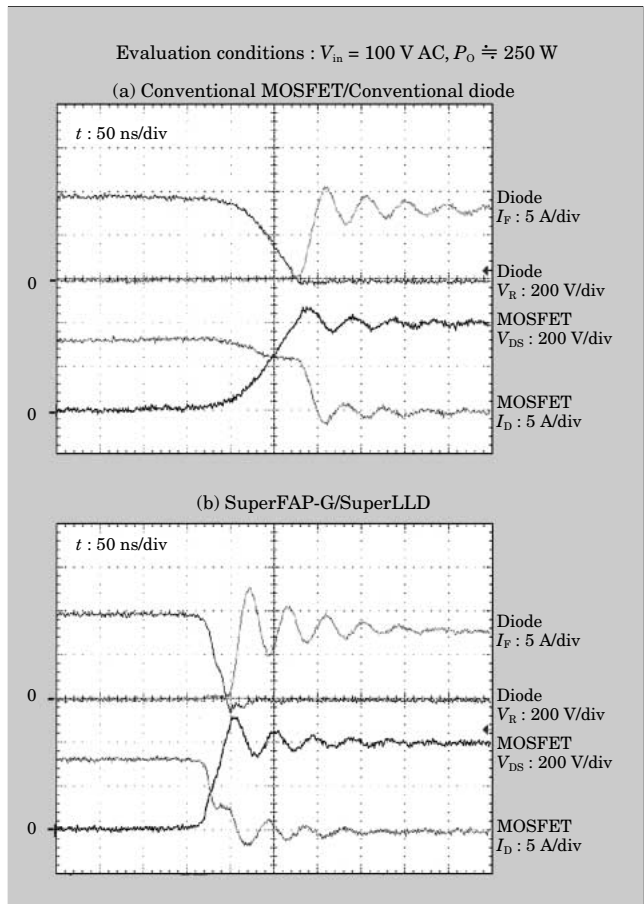
Use of the SuperFAP-G series in conjunction with the SuperLLD series in commercial SMPS equipped with continuous current mode PFC circuits resulted in an approximate 1 % improvement in efficiency and a 6 % decrease in the heat sink temperature-rise, as shown in Fig. 8 and Fig. 9.

Examples of recommended combinations of the SuperFAP-G and SuperLLD series in continuous current mode PFC circuits are listed in Table 3.

4.2 Application to DC-DC converter

Brick type DC-DC converters are used in the on-board power supplies of information and communication equipment. At present, the trends toward downsizing and increased power density are proceeding concurrently, and most leading DC-DC converters are moving away from conventional full-brick types and toward half-brick (1/2) or smaller types that have the

Fig.7 Continuous current mode PFC circuit (turn-off waveform)



same power capacity with smaller external dimensions. To achieve downsizing and power density improvement, it is necessary to downsize the passive components (such as capacitor, inductor, transformer) and reduce the switching device loss by using a higher

switching frequency.

To reduce the switching device loss, the switching loss and drive loss must be decreased, since the switching is operated at a high frequency of more than 300 kHz.

Fig.8 Continuous current mode PFC (measured results of temperature-rise)

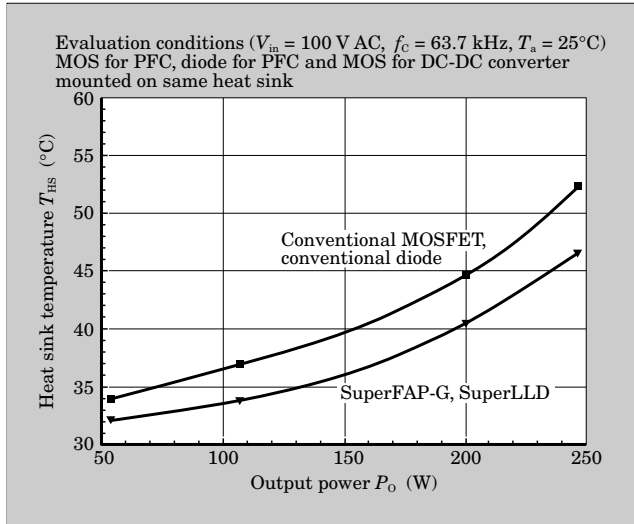


Fig.9 Continuous current mode PFC (measured results of conversion efficiency)

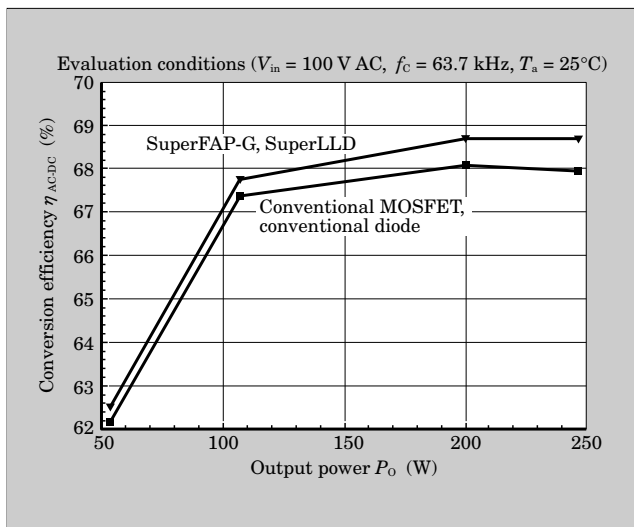


Fig. 10 Evaluation results of installation in DC-DC converter (low output)

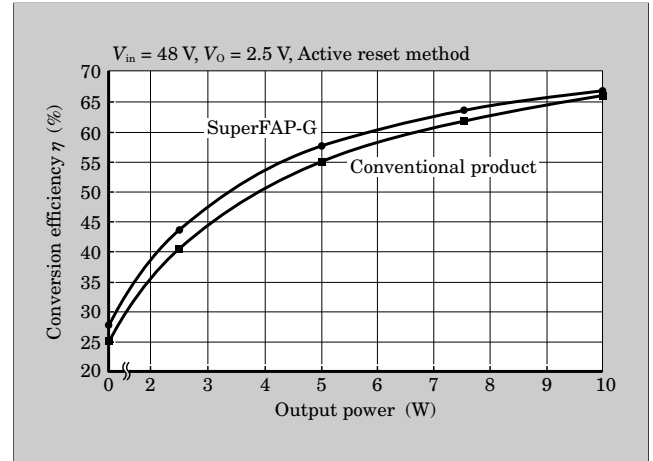


Fig.11 Evaluation result of installation in DC-DC converter (high output)

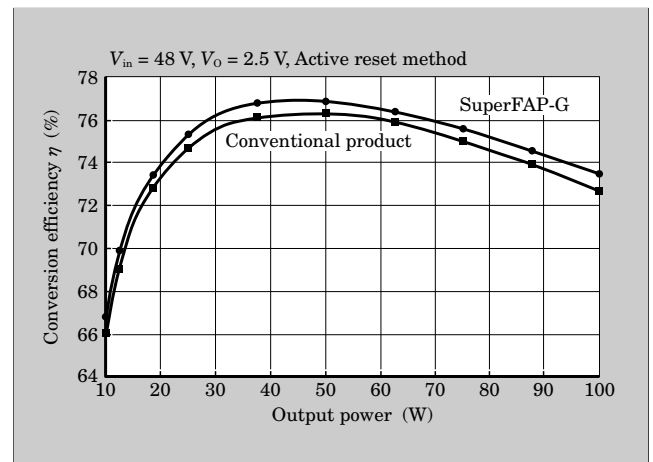


Table 3 SuperFAP-G/SuperLLD for continuous current mode PFC

Power supply capacity P_O	Model	Electrical characteristics				Package
		V_{DS}	I_D	$R_{DS(on)}$	Q_{gd}	
$\leq 150W$	2SK3504-01	$V_{DS} = 500 V$	$I_D = 14 A$	$R_{DS(on)} = 0.46 \Omega$ (max.)	$Q_{gd} = 10.5 nC$ (typ.)	TO-220
	YA961S6	$V_R = 600 V$	$I_P = 8 A$	$V_F = 2.0 V$ (typ.)	$t_{rr} = 23 ns$ (max.)	TO-220
$\leq 250W$	2SK3522-01	$V_{DS} = 500 V$	$I_D = 21 A$	$R_{DS(on)} = 0.26 \Omega$ (max.)	$Q_{gd} = 20 nC$ (typ.)	TO-247
	YA962S6	$V_R = 600 V$	$I_P = 10 A$	$V_F = 1.6 V$ (typ.)	$t_{rr} = 25 ns$ (max.)	TO-220
$\leq 350W$	2SK3680-01	$V_{DS} = 500 V$	$I_D = 43 A$	$R_{DS(on)} = 0.11 \Omega$ (max.)	$Q_{gd} = 50 nC$ (typ.)	TO-247
	YA963S6	$V_R = 600 V$	$I_P = 15 A$	$V_F = 1.7 V$ (typ.)	$t_{rr} = 30 ns$ (max.)	TO-220

Figures 10 and 11 show evaluation results of the recently developed 150 V/70 mΩ SuperFAP-G series, which was installed in a typical, commercially available quarter-brick type DC-DC converter (48 V input, 2.5 V output, 150 W).

Compared to a conventional power MOSFET with the same ratings, an approximate 60 % reduction in gate charge and a maximum 4 % improvement in conversion efficiency have been achieved. To meet the needs for downsizing, small TFP-packaged products for surface mounting are also included in the product line.

5. Conclusion

This paper has presented an overview of the design and application effect of Fuji Electric's SuperFAP-G

series of low-loss and ultra high-speed switching power MOSFETs. Application of the SuperFAP-G series to SMPS or DC-DC converters will increase conversion efficiency and reduce both power dissipation and temperature-rise. We are certain that this series will contribute to energy savings and downsizing of equipment.

In the future, Fuji Electric will work to expand this product line to meet a wider range of power supply specifications.

Reference

- (1) Kobayashi, T. et al. High-Voltage Power MOSFETs Reached Almost to the Silicon Limit. Proceedings of the 13th ISPSD. 2001, p.435-438.



Global Network



■ : Representative Office ● : Sales Bases ◆ : Manufacturing Bases

AMERICA

- **FUJI ELECTRIC CORP. OF AMERICA**
USA
Tel : +1-201-712-0555 Fax : +1-201-368-8258
- ◆ **U.S. FUJI ELECTRIC INC.**
USA
Tel : +1-732-560-9410 Fax : +1-732-457-0042
- ◆ **FUJI HI-TECH, INC.**
USA
Tel : +1-510-651-0811 Fax : +1-510-651-9070
- **FUJI SEMICONDUCTOR, INC.**
USA
Tel : +1-972-733-1700 Fax : +1-972-381-9991
- **GE FUJI DRIVES, USA INC.**
USA
Tel : +1-540-387-5925 Fax : +1-540-387-8580

EU

- **FUJI ELECTRIC CO., LTD.**
Erlangen Representative Office
F.R. GERMANY
Tel : +49-9131-729613 Fax : +49-9131-28831
- **FUJI ELECTRIC GmbH**
F.R. GERMANY
Tel : +49-69-6690290 Fax : +49-69-6661020
- **FUJI ELECTRIC UK**
U.K.
Tel : +44-208-233-1130 Fax : +44-208-233-1140
- ◆ **FUJI ELECTRIC (SCOTLAND) LTD.**
U.K.
Tel : +44-1355-234111 Fax : +44-1355-238810
- ◆ **FUJI ELECTRIC FRANCE S.A.**
FRANCE
Tel : +33-4-73-98-26-98 Fax : +33-4-73-98-26-99

ASIA

East Asia

- **FUJI ELECTRIC CO., LTD.**
China Representative Office
THE PEOPLE'S REPUBLIC OF CHINA
Tel : +86-21-6471-0897 Fax : +86-21-6471-4903
- **FUJI ELECTRIC CO., LTD.**
Beijing Representative Office
THE PEOPLE'S REPUBLIC OF CHINA
Tel : +86-10-6505-1263 Fax : +86-10-6505-1851
- **FUJI ELECTRIC (SHANGHAI) CO., LTD.**
THE PEOPLE'S REPUBLIC OF CHINA
Tel : +86-21-6466-2810 Fax : +86-21-6473-3292
- ◆ **FUJI ELECTRIC DALIAN CO., LTD.**
THE PEOPLE'S REPUBLIC OF CHINA
Tel : +86-411-762-2000 Fax : +86-411-762-2030
- ◆ **SHANDONG LUNENG FUJI ELECTRIC CO., LTD.**
THE PEOPLE'S REPUBLIC OF CHINA
Tel : +86-531-723-1138 Fax : +86-531-726-1737

- ◆ **SHANGHAI FUJI ELECTRIC SWITCHGEAR CO., LTD.**
THE PEOPLE'S REPUBLIC OF CHINA
Tel : +86-21-5718-5740 Fax : +86-21-5718-1448
- ◆ **SHANGHAI FUJI ELECTRIC TRANSFORMER CO., LTD.**
THE PEOPLE'S REPUBLIC OF CHINA
Tel : +86-21-5718-5747 Fax : +86-21-5718-5745
- ◆ **SHANGHAI GENERAL FUJI REFRIGERATION EQUIPMENT CO., LTD.**
THE PEOPLE'S REPUBLIC OF CHINA
Tel : +86-21-6921-1088 Fax : +86-21-6921-1066
- ◆ **HONG KONG FUJIDENKI CO., LTD.**
HONG KONG
Tel : +852-2664-8699 Fax : +852-2664-8040
- **FUJI ELECTRIC (ASIA) CO., LTD.**
HONG KONG
Tel : +852-2311-8282 Fax : +852-2312-0566
- **FUJI ELECTRIC CO., LTD.**
Taipei Representative Office
TAIWAN
Tel : +886-2-2561-1255 Fax : +886-2-2561-0528
- **FUJI ELECTRIC TAIWAN CO., LTD.**
TAIWAN
Tel : +886-2-2515-1850 Fax : +886-2-2515-1860
- **FUJI/GE TAIWAN CO., LTD.**
TAIWAN
Tel : +886-2-2556-0716 Fax : +886-2-2556-0717
- ◆ **ATAI FUJI ELECTRIC CO., LTD.**
TAIWAN
Tel : +886-3-321-3030 Fax : +886-3-321-7890
- **FUJI ELECTRIC KOREA CO., LTD.**
KOREA
Tel : +82-2-780-5011 Fax : +82-2-783-1707

Southeast Asia

- **FUJI ELECTRIC CO., LTD.**
Bangkok Representative Office
THAILAND
Tel : +66-2-653-2020, 2021 Fax : +66-2-653-2022
- ◆ **FUJI ELECTRIC (MALAYSIA) SDN. BHD.**
MALAYSIA
Tel : +60-4-403-1111 Fax : +60-4-403-1496
- ◆ **FUJI ELECTRIC PHILIPPINES, INC.**
PHILIPPINES
Tel : +63-2-844-6183 Fax : +63-2-844-6196
- **P. T. BUKAKA FUJI ELECTRIC**
INDONESIA
Tel : +62-21-572-4282 Fax : +62-21-572-4283
- **FUJI ELECTRIC SINGAPORE PRIVATE LTD.**
SINGAPORE
Tel : +65-479-5531 Fax : +65-479-5210
- ◆ **FUJI/GE PRIVATE LTD.**
SINGAPORE
Tel : +65-533-0010 Fax : +65-533-0021

